Onset of fluidity in two dimensions: An exact solution

A.V.Shytov

School of Physics, University of Exeter, EX4 4QL, United Kingdom

I. INTRODUCTION

Recent progress in nanofabrication and two-dimensional electronics made it possible to observe effects of fluidity in charge transport. The fluidity arises due to momentum-conserving electron-electron(ee) collisions, which become important at intermediate temperatures, and its effects become pronounced at length scales exceeding ee mean free path l_{ee}. Signatures of fluidity have been observed in many different systems, including single- and bilayer graphene, $PdCoO_2$ and WP_2, GaAs quantum wells.

An important feature of fluidity is that far away from boundaries, momentum-conserving collisions permit a finite flow of current under a negligible bias field. Finite resistivity arises mostly as a result of boundary relaxation and hence is characterised by large momentum relaxation time. Thus a well-developed fluidity can be difficult to probe by measuring electric potentials. In fact, simple dimensional estimates demonstrate that the fluidity signatures are maximal at its onset, when the electron-electron mean-free path is comparable with characteristic dimensions of the system (e.g. sample size, source-to-probe distance, etc.) Analysing this crossover regime theoretically is challenging for two reasons: boundaries play an important role, and there is no small parameter to control approximations.

In this article, we report an exact solution of the Boltzmann kinetic equation applicable in several qualitatively different regimes: in the ballistic regime, the viscous regime, as well as across the crossover between these regimes. As such the method developed in this work provides a rigorous description of the onset of fluidity. We consider kinetics of momentum-conserving collisions in a Fermi gas near a diffuse boundary and outline how one can perform a detailed quantitative analysis applicable at all length scales r. We present a general method for finding flow patterns and potential distributions in such flows and illustrate the method with several examples: we consider the flow due to current injection from the boundary or within the interior. We also consider the "Stokeslet", the flow induced by a pointlike momentum source.

The outline of the article is as follows. In Sec. II, the kinetic equation and the diffuse the boundary condition is introduced and reformulated as a problem in an infinite space involving external sources and secondary Lambertian sources due to the diffuse boundary. In Sec. III, we introduce the core concepts of the formalism. We reformulate the problem in Fourier space, and show that it can be reduced to the system of integral equations of

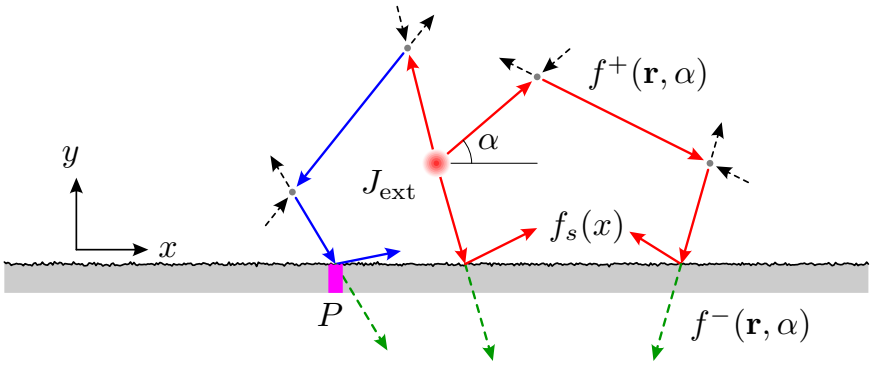

FIG. 1: Charge carriers (red arrows) are emitted by the source $J_{\rm ext}(x,y,\alpha)$ (red circle). The carriers collide with the Fermi sea background (black dashed lines). Momentum-conserving backscattering changes particles into holes (blue arrows). Propagation of charge carriers is confined to half-space ($y>0$) bounded by a rough wall (grey). Diffuse scattering by the wall can be treated as a secondary Lambertian source of intensity $f_s(x)$. The distribution of downward-moving particles can be continued to the other side of the wall (green). Hence we define the distribution function $f^+(x,y,\alpha)$ at $y>0$ and $f^-(x,y,\alpha)$ at $y<0$. The flux into the edge can be sensed by a probe P attached to it.

the Wiener-Hopf(WH) type which are almost decoupled, Eqs.(3.19)–(3.22). We derive the relation between the intensity f_s of the diffuse source and the solution of the Wiener-Hopf problem, Eq.(3.24). In Sec. IV we discuss factorisation of the kernels which is the key tool for solving the WH equations. In Sec. V, we present the general solution of the WH equations for an arbitrary source configuration. We then analyse in detail several sources of physical interest. The explicit form of the contributions of the secondary Lambertian source is derived in Sec. VI. In Sec. VII we construct a solution describing current injected from the boundary and backscattered in the bulk. The self-consistent solution that describes the vicinity-resistance geometry is obtained and discussed in Sec. VIII. Current and momentum injection in the bulk are analysed in Secs. IX and X, respectively. Conclusions and outlook are given in Sec. XI. Technical details are also discussed in Appendices.

II. THE MODEL AND ITS KINETIC EQUATION

We consider kinetics of charge carriers in a Fermi gas described by the Boltzmann equation confined to a half-plane by a boundary shown in Fig. 1. We make the follow-

ing approximations. First, we neglect energy dependence of the distribution function, so that the carrier momentum is completely characterised by the propagation angle α, see Fig. 1. (We shall refer to particles with $0 < \alpha < \pi$ as upward-going and to particles with $-\pi < \alpha < 0$ as downward-going.) This can be justified by recalling that in two dimensions energy relaxation occurs faster than momentum relaxation[1] owing to nearly collinear processes. Hence we write the distribution function of the particles in the simplified form $f(\boldsymbol{r}, \boldsymbol{p}) \approx f_{\rm eq}(\epsilon_p) - f'(\boldsymbol{r}, \alpha)\frac{\partial f_{\rm eq}}{\partial \epsilon_p}$, where ϵ_p is the carrier dispersion, and $f_{\rm eq}(\epsilon)$ is the equilibrium Fermi distribution function. (More accurately, $f'(\boldsymbol{r}, \alpha)$ can be viewed as the integral of the non-equilibrium part of the distribution function integrated over the momentum magnitude p along the ray $\boldsymbol{p} = p(\cos\alpha, \sin\alpha)$.) The quantity $f'(\boldsymbol{r}, \alpha)$ characterises the deviation of the gas from the equilibrium, and will be referred to as the distribution function through the rest of this paper. For convenience, we choose the units in which the particle's Fermi velocity and Fermi momentum are both equal to one. We write the kinetic equation in the form

$$\boldsymbol{v} \cdot \boldsymbol{\nabla} f'(\boldsymbol{r}, \alpha) = J_{\rm ext}(\boldsymbol{r}, \alpha) + I_{\rm ee}[f'(\boldsymbol{r}, \alpha)] + I_{\rm eph}[f'(\boldsymbol{r}, \alpha)] \ , \tag{2.1}$$

where $\boldsymbol{v} = (\cos\alpha, \sin\alpha)$ is particle's velocity, $J_{\rm ext}(\boldsymbol{r}, \alpha)$ describes given external sources of particles, or external fields, $I_{\rm ee}[f']$ and $I_{\rm eph}[f']$ are the electron-electron and electron-phonon collision integrals, respectively. (Eq.(2.1) does not include electric potential $\phi(\boldsymbol{r})$, its role is discussed at the end of this section.)

A simple model for momentum-preserving ee collision integral is given by[?]

$$I_{\rm ee}[f'] = -\gamma' f'(\alpha) + \gamma' \int \frac{d\alpha'}{2\pi} \left[1 + 2\cos(\alpha - \alpha')\right] f'(\alpha') \ , \tag{2.2}$$

where γ' is the interparticle collision rate. This form of $I_{\rm ee}[f']$ preserves the total particle number and the total momentum, as can be seen from the identities $I_{\rm ee}[1] = I_{\rm ee}[\cos\alpha] = I_{\rm ee}[\sin\alpha] = 0$; all other angular harmonics of $f'(\boldsymbol{r}, \alpha)$ relax at the same rate γ': $I_{\rm ee}[e^{in\alpha}] = -\gamma' e^{in\alpha}$ for $n \neq 0, \pm 1$. The collision integral (2.2) bears formal similarity to the collision integral for impurity scattering; however "the scattering probability" $\propto \gamma'(1 + 2\cos(\alpha - \alpha'))$ is negative for backward scattering $\alpha' \approx \alpha + \pi$. This reflects momentum-conserving nature of scattering, and can be interpreted as backscattering of holes in the Fermi sea background. Indeed, an incident particle propagating in the direction α' colliding with a background particle at α thus depletes the equilibrium distribution at α.

Similarly, momentum-relaxing processes can be described by

$$I_{\mathrm{e-ph}}[f'] = -\gamma'' f'(\alpha) + \gamma'' \int \frac{d\alpha'}{2\pi} f'(\alpha') \ , \tag{2.3}$$

where γ'' is the electron-phonon or electron-impurity relaxation rate. Electron-phonon collisions relax momentum, but also preserve the total number of electrons: $I_{\mathrm{e-ph}}[1] = 0$, $I_{\mathrm{e-ph}}(\cos\alpha) = -\gamma'' \cos\alpha$, etc. The full collision integral can be also rewritten in the form

$$I[f'(\boldsymbol{r},\alpha)] = I_{\mathrm{ee}}[f'] + I_{\mathrm{e-ph}}[f'] = -\gamma f'(\boldsymbol{r},\alpha) + \gamma\rho(\boldsymbol{r}) + 2\gamma' \boldsymbol{j}(\boldsymbol{r})\cdot\boldsymbol{v} \ , \tag{2.4}$$

where $\gamma \equiv \gamma' + \gamma''$ is the total relaxation rate, and the quantities

$$\rho(\boldsymbol{r}) = \langle f'(\boldsymbol{r},\alpha)\rangle \ , \qquad \boldsymbol{j}(\boldsymbol{r}) = \langle f'(\boldsymbol{r},\alpha)\boldsymbol{v}\rangle \ , \qquad \langle \dots \rangle \equiv \oint \frac{d\alpha}{2\pi} \dots \ , \tag{2.5}$$

will be referred later as the charge and current density, respectively. (They differ from true charge and current densities by the factor $e\nu$, where e is the elementary charge, and ν is the density of states.) We shall be mostly interested in purely viscous case, $\gamma'' = 0$, so that $\gamma = \gamma'$, or in the weakly ohmic regime, $\gamma'' \ll \gamma$.

Therefore, the Boltzmann equation can be written in the form

$$\boldsymbol{v}\cdot\boldsymbol{\nabla} f'(\boldsymbol{r},\alpha) + \gamma f'(\boldsymbol{r},\alpha) = J_{\mathrm{ext}}(\boldsymbol{r},\alpha) + \gamma\rho(\boldsymbol{r}) + 2\gamma'\boldsymbol{j}(\boldsymbol{r})\cdot\boldsymbol{v} \ . \tag{2.6}$$

The term $\gamma f'(\boldsymbol{r},\alpha)$ describes the decay of particles in a given momentum state due to collisions, while the terms proportional to $\rho(\boldsymbol{r})$ and $\boldsymbol{j}(\boldsymbol{r})$ describe scattered particles (and holes).

Eq.(2.6) is to be supplied with the boundary condition(b.c.) describing the scattering at the diffuse edge, $y = 0$. It is customary to describe diffuse scattering by Lambert's law which yields an isotropic distribution of upward-going particles, i.e., angle-independent $f'(x, y = 0, \alpha) = f_s(x)$. The value of $f_s(x)$ is to be determined from the charge conservation: the flux $\Phi(x)$ of downward-going particles is equal to the flux of the scattered particles f_s/π:

$$f_s(x) = \pi\Phi(x), \qquad \Phi(x) \equiv \int_{-\pi}^{0} f'(x, y = 0, \alpha)(-\sin\alpha)\frac{d\alpha}{2\pi} \ . \tag{2.7}$$

Following[3], we replace Eq.(2.6) and its b.c. (2.7) with an equivalent problem defined everywhere, $-\infty < y < \infty$. Imagine that the downward-going particles cross the interface

at $y = 0$ and continue their motion without changing the momentum direction, but decaying with the rate γ:

$$\boldsymbol{v} \cdot \boldsymbol{\nabla} f' + \gamma f' = 0 \text{ at } y < 0 \text{ and } \alpha < 0\,. \tag{2.8}$$

To replentish the drained particles, a diffuse source is placed at $y = 0$. Now the kinetic equation can be written in the whole two-dimensional space:

$$\boldsymbol{v} \cdot \boldsymbol{\nabla} f' + \gamma f' = J(\boldsymbol{r}, \alpha) + \gamma \Theta(y) \left[\rho(\boldsymbol{r}) + \frac{2\gamma'}{\gamma} \boldsymbol{j}(\boldsymbol{r}) \cdot \boldsymbol{v} \right] \,, \tag{2.9}$$

where $\Theta(y)$ is the Heaviside step function: $\Theta(y > 0) = 1$ and zero otherwise. The source term now includes the contribution of the diffuse scattering:

$$J(\boldsymbol{r}, \alpha) = J_{\text{ext}}(r, \alpha) + f_s(x) \Theta(\alpha) \sin\alpha \delta(y) \,. \tag{2.10}$$

(The angular Heaviside function $\Theta(\alpha)$ is equal to one for upward-moving particles, $0 < \alpha < \pi$ and vanishes for downward-movers, $-\pi < \alpha$ 0.) Eq.(2.9) effectively replaces charge- and momentum-conserving kinetics with kinetic of particles decaying at the rate γ. The particles are produced by known external sources $J_{\text{ext}}(\boldsymbol{r}, \alpha)$ as well as secondary sources proportional to $\rho(\boldsymbol{r})$ and $\boldsymbol{j}(\boldsymbol{r})$ in the interior, and to $f_s(x)$ at the diffuse boundary. All the secondary sources are to be determined self-consistently. This can be done by "integrating out" the microscopic degrees of freedom described by the distribution function $f'(\boldsymbol{r}, \alpha)$ and deriving integral equations relating the secondary sources $\rho(\boldsymbol{r})$, $\boldsymbol{j}(\boldsymbol{r})$, and $f_s(x)$. Solving the equations for a given $f_s(x)$ eliminates the macroscopic variables $\rho(\boldsymbol{r})$ and $\boldsymbol{j}(\boldsymbol{r})$ in the interior and provides a consistency condition from which $f_s(x)$ could be determined. This programme is implemented in this article.

While the distribution function $f'(\boldsymbol{r}, \alpha)$ is hard to probe, all other quantities introduced here are directly linked to measured quantities. Strong Coulomb repulsion that we ignored so far usually results in electrical neutrality at length scales exceeding the screening radius, so the true carrier density differs significantly from $\rho(\boldsymbol{r})$. This means that the electric potential $e\phi(\boldsymbol{r})$ compensates the chemical potential $\mu(\boldsymbol{r}) = \nu^{-1}\rho(\boldsymbol{r})$, where ν is the density of states. Thus, the density distribution can be converted into electric potential distribution: $\phi(\boldsymbol{r}) = -(\nu e)^{-1}\rho(\boldsymbol{r})$. The local electric potential can be measured e.g. by a single-electron transistor operating as a scanning gate[6]. Recently, it was also shown[9] that the current distribution $\boldsymbol{j}(\boldsymbol{r})$ can be measured indirectly, by applying a weak magnetic field and registering

the change in the local electric potential: $\phi_B(\boldsymbol{r}) = \phi(r) - eB\Psi(\boldsymbol{r})$, where $\Psi(\boldsymbol{r})$ is the stream function defined by $j_x = \partial_y \Psi$, $j_y = -\partial_x \Psi$.

Another important probe of fluidity is provided by vicinity resistance measurements[7,8]: a voltage probe is attached to the edge as shown in Fig. 1. Such a probe registers only the particles directed into the probe, and hence its signal may differ from $\phi(\boldsymbol{r})$ if the system is far from a local equilibrium. This provides an independent insight into onset of fluidity. In a simple model, the edge probe senses the flux $\Phi(x)$ of particles into the contact area akin to a Pitot's tube: $V_P \propto \Phi_0(x_P)$, where x_P is the position of the probe. Thus, the diffuse source $f_s(x) = \Phi(x)/\pi$ can be linked to edge potential measurements.

III. THE FOURIER REPRESENTATION AND THE WIENER–HOPF INTEGRAL EQUATIONS

To solve for the distribution function $f'(\boldsymbol{r}, \alpha)$ for a given configuration primary and secondary sources, we pass to the Fourier representation:

$$f'_{\boldsymbol{k}}(\alpha) \equiv \iint\limits_{-\infty}^{\infty} d^2\boldsymbol{r} f'(\boldsymbol{r}, \alpha) e^{i\boldsymbol{k}\cdot\boldsymbol{r}} \ , \qquad f'(\boldsymbol{r}, \alpha) = \iint \frac{d^2\boldsymbol{k}}{(2\pi)^2} e^{-i\boldsymbol{k}\cdot\boldsymbol{r}} f'_{\boldsymbol{k}}(\alpha) \ , \tag{3.1}$$

where $\boldsymbol{k} = (k, q)$ is a two-dimensional wave vector. In what follows, we shall use the shorthand notations: $\boldsymbol{k}^2 \equiv k^2 + q^2$, $\boldsymbol{k}\cdot\boldsymbol{v} \equiv k\cos\alpha + q\sin\alpha$, and $\boldsymbol{k}\times\boldsymbol{v} \equiv k\sin\alpha - q\cos\alpha$.

Note that the sign convention introduced in Eq.(3.1) is opposite to the one commonly used in physics literature. Our choice is commonly employed in literature on the Wiener-Hopf method (e.g.[2]) because it simplifies the connection between real-space properties of $f'(\boldsymbol{r}, \alpha)$ and complex-analytic properties of its Fourier image. Let $F(y)$ be an arbitrary function represented via its restrictions $\varphi^{\pm}$(y) to the upper and lower-half planes: $F^+(y) = \Theta(y)F(y)$, $F^-(y) = \Theta(-y)\varphi(y)$, $\varphi(y) = F^+(y) + F^-(y)$. Then the Fourier image F_q^+ of its top half $F^+(y)$, is complex-analytic at $\operatorname{Im} q > 0$, while the image F_q^- of the bottom half is analytic at $\operatorname{Im} q < 0$. This is the cornerstone principle of the Wiener-Hopf approach: one may separate contributions of two half-planes in real space by examining analytic properties of the relevant quantities in the Fourier space.

In the Fourier representation (3.1) the kinetic equation (2.9) takes the form

$$(\gamma - i\boldsymbol{k}\cdot\boldsymbol{v})f' = J_{\boldsymbol{k}}(\alpha) + \gamma\rho^+_{\boldsymbol{k}} + 2\gamma'\boldsymbol{j}^+_{\boldsymbol{k}}\cdot\boldsymbol{v} \ . \tag{3.2}$$

The scattered particle contribution is written in terms of the parts of $\rho_{\boldsymbol{k}}$ and $\boldsymbol{j}_{\boldsymbol{k}}$ that are analytic in the upper half of the complex plane q. Eq.(3.2) can be employed to determine the functions $\rho_{\boldsymbol{k}}$ and $\boldsymbol{j}_{\boldsymbol{k}}$ by calculating the relevant harmonics of the distribution function. This results in three equations which are decoupled by representing the current density $\boldsymbol{j}_{\boldsymbol{k}}$ in terms of its divergence $D_{\boldsymbol{k}} \equiv \boldsymbol{k}\cdot\boldsymbol{j}_{\boldsymbol{k}}$ and vorticity $\Omega_{\boldsymbol{k}} \equiv \boldsymbol{k}\times\boldsymbol{j}_{\boldsymbol{k}}$. (In other words, we separate the longitudinal and transverse components of $\boldsymbol{j}_{\boldsymbol{k}}$ represented by $D_{\boldsymbol{k}}$ and $\Omega_{\boldsymbol{k}}$, respectively.) Employing the identity

$$\boldsymbol{j}_{\boldsymbol{k}}\cdot\boldsymbol{v} = \frac{D_{\boldsymbol{k}}(\boldsymbol{k}\cdot\boldsymbol{v}) + \Omega_{\boldsymbol{k}}(\boldsymbol{k}\times\boldsymbol{v})}{\boldsymbol{k}^2} \ , \tag{3.3}$$

we obtain the formal solution of (3.2):

$$f'_{\boldsymbol{k}}(\alpha) = \frac{1}{\gamma - i\boldsymbol{k}\cdot\boldsymbol{v}}\left[J_{\boldsymbol{k}}(\alpha) + \gamma\rho_{\boldsymbol{k}} + \frac{2\gamma' D^+_{\boldsymbol{k}}(\boldsymbol{k}\cdot\boldsymbol{v})}{\boldsymbol{k}^2} + \frac{2\gamma'\Omega^+_{\boldsymbol{k}}(\boldsymbol{k}\times\boldsymbol{v})}{\boldsymbol{k}^2}\right] \ . \tag{3.4}$$

To determine $\rho_{\boldsymbol{k}}$, $D_{\boldsymbol{k}}$ and $\Omega_{\boldsymbol{k}}$ self-consistently, we calculate the relevant moments of the distribution function $f'_{\boldsymbol{k}}(\alpha)$, with the help of the following angular integrals:

$$\left\langle \frac{1}{\gamma - i\boldsymbol{k}\cdot\boldsymbol{v}} \right\rangle = \frac{1}{\sqrt{\gamma^2+\boldsymbol{k}^2}} \ , \qquad \left\langle \frac{\boldsymbol{k}\cdot\boldsymbol{v}}{\gamma - i\boldsymbol{k}\cdot\boldsymbol{v}} \right\rangle = i\left(1 - \frac{\gamma}{\sqrt{\gamma^2+\boldsymbol{k}^2}}\right) \ , \tag{3.5}$$

$$\left\langle \frac{(\boldsymbol{k}\cdot\boldsymbol{v})^2}{\gamma - i\boldsymbol{k}\cdot\boldsymbol{v}} \right\rangle = \gamma\left(1 - \frac{\gamma}{\sqrt{\gamma^2+\boldsymbol{k}^2}}\right) \ , \qquad \left\langle \frac{(\boldsymbol{k}\times\boldsymbol{v})^2}{\gamma - i\boldsymbol{k}\cdot\boldsymbol{v}} \right\rangle = \sqrt{\gamma^2+\boldsymbol{k}^2} - \gamma \ .$$

This leads to the system of equations:

$$\rho_{\boldsymbol{k}} = \langle f'_{\boldsymbol{k}}\rangle \qquad = \rho_{\rm dct}(\boldsymbol{k}) + \rho^+_{\boldsymbol{k}}\left[1 - K_\rho(\boldsymbol{k})\right] + \frac{2i\gamma' D^+_{\boldsymbol{k}}}{\boldsymbol{k}^2}K_\rho(\boldsymbol{k}) \ , \tag{3.6}$$

$$D_{\boldsymbol{k}} = \langle f'_{\boldsymbol{k}}(\boldsymbol{k}\cdot\boldsymbol{v})\rangle \qquad = D_{\rm dct}(\boldsymbol{k}) + i\gamma\rho^+_{\boldsymbol{k}}K_\rho(\boldsymbol{k}) + \frac{2\gamma\gamma' D^+_{\boldsymbol{k}}}{\boldsymbol{k}^2}K_\rho(\boldsymbol{k}) \ , \tag{3.7}$$

$$\Omega_{\boldsymbol{k}} = \langle f'_{\boldsymbol{k}}(\boldsymbol{k}\times\boldsymbol{v})\rangle \qquad = \Omega_{\rm dct}(\boldsymbol{k}) + \Omega^+_{\boldsymbol{k}}\left[1 - K_\Omega(\boldsymbol{k})\right] \ . \tag{3.8}$$

The kernels $K_\rho(\boldsymbol{k})$ and $K_\Omega(\boldsymbol{k})$ are defined via

$$K_\rho(\boldsymbol{k}) \equiv 1 - \frac{\gamma}{\sqrt{\gamma^2+\boldsymbol{k}^2}} \qquad = 1 - \frac{\gamma}{\sqrt{\gamma^2+k^2+q^2}} \ , \tag{3.9}$$

$$K_\Omega(\boldsymbol{k}) \equiv 1 - \frac{2\gamma'}{\boldsymbol{k}^2}\left(\sqrt{\gamma^2+\boldsymbol{k}^2} - \gamma\right) \quad = \frac{k^2+q^2+\gamma^2}{k^2+q^2}K_\rho(k,q)\left(1 - \frac{2\gamma'-\gamma}{\sqrt{k^2+q^2+\gamma^2}}\right) \ . \tag{3.10}$$

In the purely viscous case, $\gamma = \gamma'$, $K_\Omega(\boldsymbol{k})$ simplifies to $K^2_\rho(\boldsymbol{k})(\boldsymbol{k}^2+\gamma^2)/\boldsymbol{k}^2$, while in the opposite ohmic limit, $\gamma' \ll \gamma$, one finds $K_\Omega(\boldsymbol{k}) = 1$. The sources in this equation can be

viewed as a contribution of particles propagating from the source via a "direct flight", i.e. unscattered:

$$\rho_{\rm dct}(\boldsymbol{k}) \equiv \left\langle \frac{J_{\boldsymbol{k}}(\alpha)}{\gamma - i\boldsymbol{k}\cdot\boldsymbol{v}} \right\rangle \ , \tag{3.11}$$

$$D_{\rm dct}(\boldsymbol{k}) \equiv \left\langle \frac{J_{\boldsymbol{k}}(\alpha)(\boldsymbol{k}\cdot\boldsymbol{v})}{\gamma - i\boldsymbol{k}\cdot\boldsymbol{v}} \right\rangle = -i\gamma\rho_{\rm dct}(\boldsymbol{k}) + i\left\langle J_{\boldsymbol{k}}(\alpha)\right\rangle \ , \tag{3.12}$$

$$\Omega_{\rm dct}(\boldsymbol{k}) \equiv \left\langle \frac{J_{\boldsymbol{k}}(\alpha)(\boldsymbol{k}\times\boldsymbol{v})}{\gamma - i\boldsymbol{k}\cdot\boldsymbol{v}} \right\rangle \ . \tag{3.13}$$

(Note that the source term $J_{\boldsymbol{k}}(\alpha)$ here includes both the external source and the secondary source on the diffuse boundary.) The direct-flight contributions depend only upon total relaxation rate γ. Separating the components from the two half-planes, $\rho_{\boldsymbol{k}} = \rho^+_{\boldsymbol{k}} + \rho^-_{\boldsymbol{k}}$, etc we recast the equations in the form

$$K_\rho(\boldsymbol{k})\rho^+_{\boldsymbol{k}} + \rho^-_{\boldsymbol{k}} = \rho_{\rm dct}(\boldsymbol{k}) + \frac{2i\gamma' D^+_{\boldsymbol{k}}}{\boldsymbol{k}^2} K_\rho(\boldsymbol{k}) \ , \tag{3.14}$$

$$D^+_{\boldsymbol{k}} + D^-_{\boldsymbol{k}} = i\gamma K_\rho \rho^+_{\boldsymbol{k}} - i\gamma\rho_{\rm dct}(\boldsymbol{k}) + i\langle J_{\boldsymbol{k}}(\alpha)\rangle + \frac{2\gamma\gamma' D^+_{\boldsymbol{k}}}{\boldsymbol{k}^2} K_\rho(\boldsymbol{k}) \ , \tag{3.15}$$

$$K_\Omega \Omega^+_{\boldsymbol{k}} + \Omega^-_{\boldsymbol{k}} = \Omega_{\rm dct}(\boldsymbol{k}) \ . \tag{3.16}$$

By employing the density equation (3.14), one can transform the divergence equation (3.15) to make the charge conservation at $y > 0$ more explicit:

$$D^+_{\boldsymbol{k}} + D^-_{\boldsymbol{k}} = -i\gamma\rho^-_{\boldsymbol{k}} + i\langle J_{\boldsymbol{k}}(\alpha)\rangle \ . \tag{3.17}$$

The quantity on the right-hand side of this relation equals to the total current injected into the system by the sources.

In real space, Eqs.(3.14)-(3.17) become integral equations with non-local kernels defined by $K_{\rho,\Omega}(\boldsymbol{k})$. In the Fourier space, they take a particularly simple form: all kernels act multiplicatively on the respective Fourier harmonics. Hence the equations can be treated with the help of the Wiener-Hopf method. This simplification is made possible by employing the diffuse boundary condition. (For a finite edge diffusivity, the equations retain a nonlocal form in the Fourier space.)

In these equations, the vorticity $\Omega_{\boldsymbol{k}}$ appears to be fully decoupled from the particle density $\rho_{\boldsymbol{k}}$ and the current divergence $D_{\boldsymbol{k}}$. However, there is also an implicit relation between the divergence and vorticity. Consider Eq. (3.3) with two arbitrary functions $D_{\boldsymbol{k}} = D^+_{\boldsymbol{k}}$ and $\Omega_{\boldsymbol{k}} = \Omega^+_{\boldsymbol{k}}$ that are complex-analytic in the upper half plane. In general, the respective

current components,

$$j_{x,\boldsymbol{k}} = \frac{D^+_{\boldsymbol{k}} k - \Omega^+_{\boldsymbol{k}} q}{k^2+q^2} \quad \text{and} \quad j_{y,\boldsymbol{k}} = \frac{D^+_{\boldsymbol{k}} q + \Omega^+_{\boldsymbol{k}} k}{k^2+q^2} \tag{3.18}$$

are *not* complex-analytic at $\operatorname{Im} q > 0$ due to a potential pole that may occur at $q = i|k|$. Hence $j_{x,y}(y<0) \neq 0$ for generic $D^+_{\boldsymbol{k}}$ and $\Omega^+_{\boldsymbol{k}}$. To suppress the unwanted pole, one must impose the following consistency condition:

$$D^* = i \operatorname{sgn} k \Omega^* \ , \tag{3.19}$$

where $D^* \equiv D^+_{\boldsymbol{k}}(q = i|k|)$ and $\Omega^* \equiv \Omega^+_{\boldsymbol{k}}(q = i|k|)$. (Various quantities evaluated at $q = i|k|$ are ubiquitous in what follows, and we shall use this notation systematically.)

Thus, to eliminate the interior variables, one has to solve the Wiener-Hopf equations

$$K_\rho(\boldsymbol{k})\rho^+_{\boldsymbol{k}} + \rho^-_{\boldsymbol{k}} = \rho_{\rm dct}(\boldsymbol{k}) + \frac{2i\gamma' D^+_{\boldsymbol{k}}}{\boldsymbol{k}^2} K_\rho(\boldsymbol{k}) \tag{3.20}$$

$$D^+_{\boldsymbol{k}} + D^-_{\boldsymbol{k}} = -i\gamma\rho^-_{\boldsymbol{k}} + i\langle J_{\boldsymbol{k}}(\alpha)\rangle \ , \tag{3.21}$$

$$K_\Omega \Omega^+_{\boldsymbol{k}} + \Omega^-_{\boldsymbol{k}} = \Omega_{\rm dct}(\boldsymbol{k}) \ , \tag{3.22}$$

for given source terms $\rho_{\rm dct}(k,q)$, $\Omega_{\rm dct}(k,q)$, together with the consistency condition (3.19). However, the system (3.19)–(3.22) is not yet closed: its right-hand side includes the unknown intensity $f_s(x)$ of the diffuse source at the boundary. The latter is to be determined by matching particle fluxes across the interface $y = 0$ as per Eq.(2.7). While the particle flux $\Phi(x)$, or its Fourier harmonic $\Phi(k)$, can be calculated from the distribution function $f'(\boldsymbol{r},\alpha)$ expressed via $\rho(\boldsymbol{r})$ and $\boldsymbol{j}(\boldsymbol{r})$, this results in rather cumbersome expressions. This, however, is obviated by making the following observation. The flux of downward-going particles is continuous across the interface and coincides with the vertical current density j_y at $y = -0$. Therefore, its Fourier image can be calculated via

$$\Phi_k = -j_{y,k}(y=0) = \int\limits_{-\infty}^{\infty} \frac{dq}{2\pi} \frac{qD^-_{\boldsymbol{k}} - k\Omega^-_{\boldsymbol{k}}}{k^2+q^2} \ . \tag{3.23}$$

The functions $D^-_{\boldsymbol{k}}$ and $\Omega^-_{\boldsymbol{k}}$ are complex-analytic at $\operatorname{Im} q < 0$, and we will see later that the integrand in this equation decays faster than $1/q$. Hence the integral can be found by closing the integration contour in the lower half-plane and evaluating the contribution of the pole at $q = -i|k|$. Balancing this flux by the diffuse source at the edge, we rewrite the flux conservation condition (2.7) in the form

$$f_s(k) = \pi\Phi(k) = -\pi J_y(-0) = \frac{\pi}{2} \left(iD^-_{\boldsymbol{k}} + \Omega^-_{\boldsymbol{k}} \operatorname{sgn} k \right)\Big|_{q=-i|k|} \ . \tag{3.24}$$

This fully eliminates microscopic degrees of freedom, both in the interiour and on the edge, and thereby closes the system (3.19)–(3.22). An interesting feature of the resulting equations is the decoupling of vorticity in the bulk, so that it is generated only by the boundaries and sources. Thus conservation of vorticity known from fluid mechanics is in fact obeyed at all scales.

IV. COMPLEX-ANALYTIC PROPERTIES OF THE KERNEL AND ITS FACTORISATION

The key ingredient of the Wiener-Hopf method is factorisation of the kernels into components with desired complex-analytic properties. Consider the kernels (3.9) and (3.10) that define the density and vorticity via Eqs.(3.20) and (3.22). The kernel $K_\rho(k,q)$ exhibits zeros at $q=\pm i|k|$ and branch cuts from $q=\pm i\kappa$ to infinity, where $\kappa\equiv\sqrt{k^2+\gamma^2}$, as shown in Fig. 2(a). The kernel $K_\Omega(k,q)$ exhibits the same branch cut and zeros at $q=i\tilde{\kappa}$, with $\tilde{\kappa}\equiv\sqrt{k^2+4\gamma'\gamma''}$. In the purely viscous case ($\gamma''=0$), the kernels exhibit singularities at identical points. The kernels also tend to one at $|q|\to\infty$. In the Wiener-Hopf approach, it is customary to seek a factorisation of the form

$$K_\rho(k,q)=\frac{K_\rho^-(k,q)}{K_\rho^+(k,q)}\ ,\qquad K_\Omega(k,q)=\frac{K_\Omega^-(k,q)}{K_\Omega^+(k,q)}\ , \tag{4.1}$$

where $K^+_{\rho,\Omega}(k,q)$ are complex-analytic at $\operatorname{Im} q>0$, while $K^-_{\rho,\Omega}(k,q)$ are analytic at $\operatorname{Im} q<0$. Besides that, the kernels $K^\pm_{\rho,\Omega}(k,q)$ should have no zeroes at in the respective half-plane. To make the factorisation unique, we also demand $K^\pm_{\rho,\Omega}(q\to\infty)=1$. In the viscous limit, $\gamma=\gamma'$, if the factorisation is known for $K_\rho(k,q)$, the factorisation for $K_\Omega(k,q)$ is also known:

$$K_\Omega^+(k,q,\gamma'=\gamma)=\left[K_\rho^+(k,q)\right]^2\frac{q+i|k|}{q+i\kappa}\ . \tag{4.2}$$

Eqs.(4.1) is a simple example of the Riemann-Hilbert problem, and its solution is provided by two Cachy integrals:

$$\log K_\rho^\pm(k,q)=\int\limits_{-\infty}^{\infty}\frac{dq'}{2\pi i}\frac{\log K_\rho(k,q')}{q-q'\pm i0}\ . \tag{4.3}$$

Indeed, each of the integrals defines a function that is complex-analytic at $\operatorname{Im} q>0$ or $\operatorname{Im} q<0$ respectively, and decays as $1/q$. Their difference on the real axis is given by $-\log K_\rho(k,q)$ by virtue of the Sokhotzky-Plemelj formula: $\operatorname{Im}(q\pm i0)^{-1}=\mp\pi\delta(q)$.

The functions $K_\rho^\pm(k,q)$ can be also continued to $\mathrm{Im}\, q < 0$ and $\mathrm{Im}\, q > 0$, respectively, via Eq.(4.1). As a result, the kernels $K_{\rho,\Omega}^+(k,q)$ inherit the singularities of $K_{\rho,\Omega}(k,q)$ in the lower half-plane, while the functions $K_{\rho,\Omega}^-(k,q)$ take care of the singularities in the upper half-plane. Therefore the function $K_\rho^+(k,q)$ must exhibit a pole at $q=-i|k|$ and a branch cut at $q=-is$, $s>\kappa$, see Fig. 2(b). The function $K_\rho^-(k,q)$ has a zero at $q=i|k|$, and is discontinuous across the branch cut $q=is$, $s>\kappa$, see Fig.2(c). The behaviour of $K_\Omega^-(k,q)$ is similar: it vanishes at $q=i\tilde{\kappa}$, and is discontinuous across the same cut. Since the kernels are even functions of q, one may also notice the following relations:

$$\overline{K_{\rho,\Omega}^+}(k,q) = \frac{1}{K_{\rho,\Omega}^-(k,\overline{q})}\ , \qquad K_{\rho,\Omega}^+(k,-q) = \frac{1}{K_{\rho,\Omega}^-(k,q)}\ , \tag{4.4}$$

where $\overline{z}$ is the complex conjugate of z. On the imaginary axis $z=is$ the functions $K_{\rho,\Omega}^\pm(k,is)$ are real-valued, and obey the relation $K_{\rho,\Omega}^-(k,-is) = 1/K_{\rho,\Omega}^+(k,is)$. Thus, all the quantities on the imaginary axis can be expressed in terms of only two non-singular functions, $K_{\rho,\Omega}^+(k,is)$ at $s>0$.

Since the only singularities of the factorised kernels $K_{\rho,\Omega}^\pm(k,q)$ occur on the imaginary axis, the contours in complex integrals involving the kernels can be transformed by pulling them up or down, see Fig.2(b, c) as one sees fit. When a contour is pulled away from the real axis, it can be caught by a pole or a cut, so that all physical quantities can in principle be expressed via the residues at the poles and an integral over the cut. In Appendix F, we give explicit expressions for the pertinent residues at the poles and discontinuities across the cuts, see Eqs. (F3) and (F4). In numerical similations, we evaluate complex integrals using the contours $C_\pm$ shown in Fig. 2(b, c) which are kept away from the singularities so that the integrands are smooth along the contours. Expressions for factorised kernels and their derivatives can be found in Appendix C.

V. SOLVING THE WIENER-HOPF EQUATIONS FOR GENERIC SOURCES

We shall now show how to solve the nonlocal equations (3.20)–(3.22), (3.19) via the Wiener-Hopf method. While the specific solutions are to be derived from the specific form of the sources $\rho_{\mathrm{dct}}(\boldsymbol{k})$, $\Omega_{\mathrm{dct}}(\boldsymbol{k})$, some conclusions and general relations can be derived for generic sources. We begin our analysis with the continuity equation (3.21), which can be

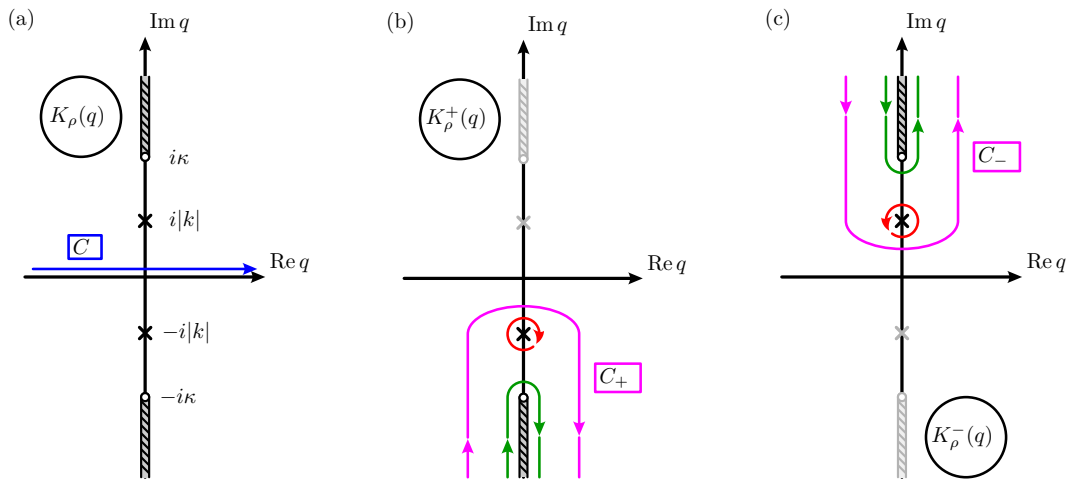

FIG. 2: The singularities and integration contours for the nonlocal kernel $K_\rho(k,q)$. (a) The kernel exhibits two zeros at $q=\pm i|k|$ and two branching points at $q=\pm i\kappa$. The respective branch cuts connect these points to infinity. The Wiener-Hopf problem is defined on the real axis; the Fourier and Cauchy integrals are to be taken along the horizontal contour shown in blue. (b) The kernel $K_\rho^+(k,q)$ has the singularities in the lower half-plane $\mathrm{Im}\, q<0$ while the singularities in the upper half-plane shown in pale gray are suppressed. In expressions involving $K_\rho^+(k,q)$ the contour C can be deformed into the path C_+ (magenta) enclosing these singularities. This path can be further transformed into a sum of a contour encircling the pole (red) and a path going around the cut (green). (c) The kernel $K_\rho^-(k,q)$ exhibits singularities in the upper half plane, so that the integration path C can be transformed into C_- which again can be reduced to the contribution of the pole and the cut.

rewritten in the form

$$D_{\boldsymbol{k}}^- + i\gamma\rho_{\boldsymbol{k}}^- = -D_{\boldsymbol{k}}^+ + i\langle J_{\boldsymbol{k}}(\alpha)\rangle\ . \tag{5.1}$$

The left-hand side is analytic in the lower half-plane, $\mathrm{Im}\, q<0$, while the right-hand side is analytic in the upper half plane $\mathrm{Im}\, q>0$. Hence they are both equal to a function analytic everywhere. Since the quantities entering Eq.(5.1) cannot grow with q, we conclude that both sides must be equal to an unknown constant C_D:

$$D_{\boldsymbol{k}}^+ = i\langle J_{\boldsymbol{k}}(\alpha)\rangle - C_D\ , \qquad D_{\boldsymbol{k}}^- + i\gamma\rho_{\boldsymbol{k}}^- = C_D\ . \tag{5.2}$$

We see that the current divergence at $y>0$ differs from the current emitted by the sources, $\langle J_{\boldsymbol{k}}(\alpha)\rangle$ by C_D. Therefore the constant C_D defines the flux of downward-moving particles through the diffuse boundary at $y=0$: $C_D(k)=i\Phi_k$, which is also consistent with the

expression for $D^-_{\boldsymbol{k}}$: the particles supplied by the source Φ_k they decay in the lower half-space. This observation has two consequences. Firstly, substituting $D^-_{\boldsymbol{k}}$ from Eq.(5.2) into Eq.(3.24), we can solve for Φ_k and thus rewrite the equation for $f_{s,k}$, relating it to the density and vorticity at $y < 0$:

$$f_{s,k} = \pi\Phi_k = \pi \left(\gamma\rho^-_{\boldsymbol{k}} - \operatorname{sgn} k\Omega^-_{\boldsymbol{k}}\right)\big|_{q=-i|k|} \ . \tag{5.3}$$

Secondly, since the current produced by the diffuse source is compensated by the flux, the divergence at $y > 0$ is in fact proportional to the current supplied by external sources only:

$$D^+_{\boldsymbol{k}} = i\langle J_{\mathrm{ext},\boldsymbol{k}}(\alpha)\rangle \ , \tag{5.4}$$

which simplifies further analysis: one may retain the contribution of D^+_k only for the external sources and drop it for the boundary scattering.

Consider now Eq. (3.20) which defines particle density. To separate the contributions of the two semispaces, we employ the factorisation (4.1) and divide both sides by $K^-_\rho(k,q)$:

$$\frac{\rho^+_{\boldsymbol{k}}}{K^+_\rho(k,q)} + \frac{\rho^-_{\boldsymbol{k}}}{K^-_\rho(k,q)} = \frac{\rho_{\mathrm{dct}}(k,q)}{K^-_\rho(k,q)} - \frac{2\gamma'\langle J_{\mathrm{ext}}(k,q)\rangle}{(k^2+q^2)K^+_\rho(k,q)} \tag{5.5}$$

To obtain the solution, one has to represent the right-hand side as a sum of two functions each analytic in the respective half-plane. This can be done explicitly for the second term. Indeed, the function $\langle J_{\mathrm{ext}}(k,q)\rangle$ represents the contributions of sources at $y \geq 0$, and hence is complex-analytic at $\operatorname{Im} q > 0$. Therefore, the only singularity in this term at $\operatorname{Im} q > 0$ is the pole at $q = i|k|$ which can be easily separated:

$$-\frac{2\gamma'\langle J_{\mathrm{ext}}(k,q)\rangle}{(k^2+q^2)K^+_\rho(k,q)} = \left[-\frac{2\gamma'\langle J_{\mathrm{ext}}(k,q)\rangle}{(k^2+q^2)K^+_\rho(k,q)} + \frac{\gamma' J^*_{\mathrm{ext}}}{|k|(|k|+iq)K^*_\rho}\right] - \frac{\gamma' J^*_{\mathrm{ext}}}{|k|(|k|+iq)K^*_\rho} \ , \tag{5.6}$$

where $J^*_{\mathrm{ext}} \equiv \langle J_{\mathrm{ext}}\rangle_{q=i|k|}$ In this expression, the first contribution is analytic everywhere at $\operatorname{Im} q > 0$ as the pole residue is suppressed, while the second term is analytic at $\operatorname{Im} q < 0$. We also represent the term proportional to $\rho_{\mathrm{dct}}(k,q)$ as

$$S^+_\rho(k,q) + S^-_\rho(k,q) = \frac{\rho_{\mathrm{dct}}(k,q)}{K^-_\rho(k,q)} \ , \tag{5.7}$$

where the functions $S^\pm_\rho(k,q)$ are complex-analytic in the respective half-planes and decay at $q \to \infty$. Regrouping the terms in Eq.(5.5) and applying the usual Wiener-Hopf reasoning,

one obtains its solution:

$$\rho^+_{\boldsymbol{k}} = K^+_\rho(k,q)S^+_\rho(k,q) - \frac{2\gamma'}{k^2+q^2}\langle J_{\rm ext}(k,q)\rangle + \frac{\gamma' J^*_{\rm ext}}{|k|(|k|+iq)}\frac{K^+_\rho(k,q)}{K^*_\rho} \ , \tag{5.8}$$

$$\rho^-_{\boldsymbol{k}} = K^-_\rho(k,q)S^-_\rho(k,q) - \frac{\gamma' J^*_{\rm ext}}{|k|(|k|+iq)}\frac{K^-_\rho(k,q)}{K^*_\rho} \ . \tag{5.9}$$

(An arbitrary constant in the Wiener-Hopf solution is fixed by the requirement $S^\pm_\rho(q \to \infty) = 0$.)

In general, when particles are emitted by point sources, one should expect a singularity at the source. To single it out, one may express $\rho^+_{\boldsymbol{k}}$ in terms of $S^-_\rho(k,q)$:

$$\rho^+_{\boldsymbol{k}} = \frac{\rho_{\rm dct}(k,q)}{K_\rho(k,q)} - \frac{2\gamma'}{k^2+q^2}\langle J_{\rm ext}(k,q)\rangle - K^+_\rho(k,q)S^-_\rho(k,q) + \frac{\gamma' J^*_{\rm ext}}{|k|(|k|+iq)}\frac{K^+_\rho(k,q)}{K^*_\rho(k)} \ . \tag{5.10}$$

The first two terms in this solution give the induced density $\rho_\infty(k,q)$ had the source $\rho_{\rm dct}(k,q)$ been placed in an infinite medium:

$$\rho_\infty(k,q) \equiv \frac{\rho_{\rm dct}(k,q)}{K_\rho(k,q)} - \frac{2\gamma'}{k^2+q^2}\langle J_{\rm ext}(k,q)\rangle \ , \tag{5.11}$$

while the last two terms represent the effect of the wall which is expected to be regular near the source. Thus, one may write

$$\delta\rho^+(k,q) = \rho_\infty(k,q) + \delta\rho_{\rm reg}(k,q) \ , \tag{5.12}$$

where the regular part $\delta\rho_{\rm reg}(k,q)$ is gven by

$$\delta\rho_{\rm reg}(k,q) = -K^+_\rho(k,q)S^-_\rho(k,q) + \frac{\gamma' J^*_{\rm ext}}{|k|(|k|+iq)}\frac{K^+_\rho(k,q)}{K^*_\rho(k)} \ . \tag{5.13}$$

The infinite-space solution $\rho_\infty(k,q)$ can be found by solving the kinetic equation in the Fourier space. Another representation of $\rho^+(k,q)$ can be obtained by noticing that the real-space singularity of $\rho^+(x,y)$ is given by $\rho_{\rm dct}(x,y)$. Singling out this term, one may also write

$$\rho^+(k,q) = \rho_{\rm dct}(k,q) + \delta\rho_\infty(k,q) + \delta\rho_{\rm reg}(k,q) \ , \tag{5.14}$$

with the excess density $\delta\rho_\infty(k,q)$ in an infinite space due to rescattered particles is given by

$$\delta\rho_\infty(k,q) = \left[\frac{1}{K_\rho(k,q)} - 1\right]\rho_{\rm dct}(k,q) - \frac{2\gamma' J_{\rm ext}(k,q)}{k^2+q^2} \ . \tag{5.15}$$

(In the real space, this contribution exhibits a weaker logarithmic singularity at the current source.) The advantage of using the representation (5.15) is that the form of $\rho_{\rm dct}(x,y)$ in the real space is often self-evident, as will be discussed later.

We now see that the density behaviour both above and below the boundary is described in terms of a single unknown function $S^-_\rho(k,q)$. In the most general case, the decomposition (5.7) can be achieved via the Cauchy integral:

$$S^-_\rho(k,q) = \int\limits_{-\infty}^{\infty} \frac{dq'}{2\pi i} \frac{\rho_{\rm dct}(k,q')}{(q-q'-i0)K^-_\rho(q')} \ , \tag{5.16}$$

in which one may shift the contour to the upper half-space so that it encloses the pole at $q=i|k|$ and the cut originating at $q=i\kappa$, see Fig.2. For the boundary sources, however, it can be found by inspecting the complex-analytic properties of the source $\rho_{\rm dct}(k,q)$ as will be shown in Secs. VI and VII.

Eq.(3.22) for vorticity is solved similarly: it is first brought to the form

$$\frac{\Omega^+_{\boldsymbol{k}}}{K^+_\Omega(k,q)} + \frac{\Omega^-_{\boldsymbol{k}}}{K^-_\Omega(k,q)} = \frac{\Omega_{\rm dct}(k,q)}{K^-_\Omega(k,q)} \ . \tag{5.17}$$

Then, the right-hand side is represented via two functions, each analytic in the respective half-plane:

$$S^+_\Omega(k,q) + S^-_\Omega(k,q) = \frac{\Omega_{\rm dct}(k,q)}{K^-_\Omega(k,q)} \ . \tag{5.18}$$

Acting as before, one writes

$$\Omega^+_{\boldsymbol{k}} = K^+_\Omega(k,q)\left[S^+_\Omega(k,q) + C_\Omega\right] \ , \tag{5.19}$$

$$\Omega^-_{\boldsymbol{k}} = K^-_\Omega(k,q)\left[S^-_\Omega(k,q) - C_\Omega\right] \ , \tag{5.20}$$

where C_Ω is an unknown constant. The key difference in this case is that the constant cannot be determined by analysing the behaviour of $\Omega_{\boldsymbol{k}}$ at $q\to\infty$. (Indeed, unlike the density $\rho_{\boldsymbol{k}}$, the vorticity tends to a finite limit at large q. In the real space, this is represented by a delta-like contribution which is related to the current density $j_x(x)$ at the edge: $\Omega(x,y) = j_x(x)\delta(y) + \Omega_{\rm reg}(x,y)$, where $\Omega_{\rm reg}(x,y)$ is regular.) Instead, the constant C_Ω is determined from the consistency condition, Eq. (3.19). This gives

$$\Omega^+(k,q) = K^+_\Omega(k,q)\left[S^+_\Omega(k,q) - S^*_\Omega(k) + \frac{J^*_{\rm ext}(k)}{K^*_\Omega(k)}\,\mathrm{sgn}\,k\right] \ , \tag{5.21}$$

$$\Omega^-(k,q) = K^-_\Omega(k,q)\left[S^-_\Omega(k,q) + S^*_\Omega(k) - \frac{J^*_{\rm ext}(k)}{K^*_\Omega(k)}\,\mathrm{sgn}\,k\right] \ , \tag{5.22}$$

where $S^*_\Omega(k) \equiv S^+_\Omega(k, q = i|k|)$. Similarly to Eq.(5.10), the singularity at the source can be separated, so that the vorticity is expressed in terms of the quantity $S^-_\Omega(k,q) + S^*_\Omega(k)$ alone:

$$\Omega^+(k,q) = \Omega_{\rm dct}(k,q) + \delta\Omega_\infty(k,q) + \delta\Omega_{\rm req}(k,q) \ , \tag{5.23}$$

with the infinite-space contribution

$$\delta\Omega_\infty(k,q) = \left[\frac{1}{K_\Omega(k,q)} - 1\right] \Omega_{\rm dct}(k,q) \ , \tag{5.24}$$

and the regular term

$$\delta\Omega_{\rm reg}(k,q) = \frac{J^*_{\rm ext}(k) K^+_\Omega(k,q)}{K^*_\Omega(k)} \operatorname{sgn} k - K^+_\Omega(k,q) \tilde{S}_\Omega(k,q) \ . \tag{5.25}$$

Here we absorbed the constant $S^*_\Omega(k)$ into the function S^-_Ω by introducing $\tilde{S}_\Omega(k,q) = S^-_\Omega(k,q) + S^*_\omega(k)$. The latter can be obtained as a difference between the respective Cauchy integrals:

$$\tilde{S}_\Omega(k,q) = \int\limits_{-\infty}^{\infty} \frac{dq'}{2\pi i} \frac{(i|k| - q)\, \Omega_{\rm dct}(k,q')}{(q - q' - i0)(i|k| - q' - i0) K^-_\Omega(k,q')} \ . \tag{5.26}$$

This integral is convergent even for $\Omega_{\rm dct}(k,q)$ tending to a non-zero limit at $q' \to \infty$, which is often the case.

Our solutoin can be also employed to calculate the flux through the edge. Substituting Eqs.(5.9) and (5.22) into Eq. (5.3), one finds

$$\begin{aligned} \Phi(k) = {} & \frac{J^*_{\rm ext}(k)}{\left[K^*_\Omega(k)\right]^2} - \frac{\gamma\gamma' J^*_{\rm ext}(k)}{2k^2 \left[K^*_\rho(k)\right]^2} + \frac{\gamma}{K^*_\rho(k)} \int\limits_{-\infty}^{\infty} \frac{dq}{2\pi} \frac{\rho_{\rm dct}(k,q)}{(|k| - iq) K^-_\rho(k,q)} \\ & - \frac{2|k|}{K^*_\Omega(k)} \int\limits_{-\infty}^{\infty} \frac{dq}{2\pi} \frac{\Omega_{\rm dct}(k,q)}{(k^2 + q^2) K^-_\Omega(k,q)} \ . \end{aligned} \tag{5.27}$$

Thus, the relations (5.13)-(5.16) and (5.23)-(5.27) give the general the solution of the Wiener-Hopf problem specified by the quantities $\rho_{\rm dct}(k,q)$, $\Omega_{\rm dct}(k,q)$ via the Cauchy integrals. The source terms $\rho_{\rm dct}(k,q)$ and $\Omega_{\rm dct}(k,q)$ include the contributions of both the external sources and the secondary source that represents diffuse scattering. This solution can be employed to deduce the intensity of the diffuse source $f_s(k)$ self-consistently, via the relation $\Phi(k) = f_s(k)/\pi$, as we shall demonstrate later.

When seeking for specific solutions to the Wiener-Hopf equations (3.20)-(3.22) one may also bear in mind how it varies when the sources at the boundary are modified for downward-moving particles, $-\pi < \alpha < 0$. The extra source, $\Delta J_k^-(\alpha)$ would produce the particles that move to the lower semispace and decay there without being backscattered into the upper semispace. Thus, the extra sources would affect $\rho_{\boldsymbol{k}}^-$ and $\Omega_{\boldsymbol{k}}^-$, but not $\rho_{\boldsymbol{k}}^+$ and $\Omega_{\boldsymbol{k}}^+$. This can be seen from the Wiener-Hopf equations: the extra sources would give rise to an extra contribution to $\rho_{\rm dct}(\boldsymbol{k})$ and $\Omega_{\rm dct}(\boldsymbol{k})$:

$$\Delta\rho^-{}_{\rm dct}(\boldsymbol{k}) = \int\limits_{-\pi}^{0} \frac{J_k^-(\alpha)}{\gamma - i\boldsymbol{k}\cdot\boldsymbol{v}} \frac{d\alpha}{2\pi} \ , \qquad \Delta\Omega^-{}_{\rm dct}(\boldsymbol{k}) = \int\limits_{-\pi}^{0} \frac{\boldsymbol{k}\times\boldsymbol{v} J_k^-(\alpha)}{\gamma - i\boldsymbol{k}\cdot\boldsymbol{v}} \frac{d\alpha}{2\pi} \ . \tag{5.28}$$

These contributions are indeed complex-analytic in the lower half-plane as all the poles of the integrand lie in the upper half plane. Thus, the extra sources (5.28) can be easily incorporated into the solution by making a trivial shift: $\rho^-(\boldsymbol{k}) \to \rho^-(\boldsymbol{k}) + \Delta\rho^-{}_{\rm dct}(\boldsymbol{k})$ etc, which does not affect the distributions at $y \geq 0$. However, such a change modifies the expression for the down-going flux due to the particles produced by the source. This yields the expression for the flux Φ_k that should be employed in the self-consistency condition:

$$\Phi_k = \left(\gamma\rho_{\boldsymbol{k}}^- - \Omega_{\boldsymbol{k}}^-\right)\big|_{q=i|k|} - \Delta\Phi_k \ , \qquad \text{with} \qquad \Delta\Phi_k = \int\limits_{-\pi}^{0} \Delta J_k^-(\alpha)\frac{d\alpha}{2\pi} \ . \tag{5.29}$$

This symmetry of the Wiener-Hopf equations allows one to choose the source terms in such a form as to simplify the analysis, as we shall see in the following two sections.

VI. THE DIFFUSE SCATTERING CONTRIBUTION

We can now discuss the explicit form of the diffuse contribution. To this end, we extend the Lambertian source antisymmetrically to down-going angles, writing the source in Eq. (2.6) the form $J_s(\alpha, x, y) = f_s(x)\sin\alpha\delta(y)$, which is rewritten in the Fourier space as $J_s(\alpha, k, q) = f_s(k)\sin\alpha$. (An alternative treatment in which the source is not extended to negative angles is given in Appendix A.) Evaluating the integrals (3.11) and (3.13), one may express the results in terms of the kernels $K_{\rho,\Omega}(k, q)$:

$$\rho_{\rm dct}^{\rm (diff)}(k, q) = \frac{iqf_s(k)}{k^2+q^2} K_\rho(k, q) \ , \qquad \Omega_{\rm dct}^{\rm (diff)}(k, q) = \frac{kf_s(k)}{2\gamma'} \left[1 - K_\Omega(k, q)\right] \ . \tag{6.1}$$

The extra flux $\Delta\Phi_k$ supplied by the extended source in the downward direction is equal to $-f_s(k)/\pi$. Since we do not treat the diffuse scattering as a source of external current, the current term in the density equation (3.20) can be suppressed. Hence the source term in the density equation takes the form

$$S_\rho^+(k,q) + S_\rho^-(k,q) = \frac{iqf_s(k)}{q^2+k^2}\frac{1}{K_\rho^+(k,q)} \ . \tag{6.2}$$

Instead of computing the Cauchy integral (5.16), one can simply separate the pole at $q = i|k|$ as before:

$$S_\rho^+(k,q) = \frac{iqf_s(k)}{q^2+k^2}\frac{1}{K_\rho^+(k,q)} + \frac{1}{2(|k|+iq)}\frac{1}{K_\rho^*(k)} \ , \tag{6.3}$$

$$S_\rho^-(k,q) = -\frac{f_s(k)}{2(|k|+iq)}\frac{1}{K_\rho^*(k)} \ . \tag{6.4}$$

Similarly, the source in the vorticity equation (3.22) can be recast as

$$S_\Omega^+(k,q) + S_\Omega^-(k,q) = \frac{kf_s(k)}{2\gamma'}\left[\frac{1}{K_\Omega^-(k,q)} - \frac{1}{K_\Omega^+(k,q)}\right] \ . \tag{6.5}$$

Obviously, the first term contributes to $S_\Omega^-(k,q)$ while the second term gives rise to S_Ω^+. The constant term is derived from the self-consistency condition (3.19), so that

$$S_\Omega^+(k,q) = \frac{kf_s(k)}{2\gamma'}\left[\frac{1}{K_\Omega^*(k)} - \frac{1}{K_\Omega^+(k,q)}\right] \ , \tag{6.6}$$

$$S_\Omega^-(k,q) = \frac{kf_s(k)}{2\gamma'}\left[-\frac{1}{K_\Omega^*(k)} + \frac{1}{K_\Omega^-(k,q)}\right] \ .$$

Thus, one finds for the physical density and vorticity:

$$\rho^{(\mathrm{diff})}(k,q) = f_s(k)\rho_s(k,q) \ , \qquad \rho_s(k,q) \equiv \left[\frac{iq}{q^2+k^2} + \frac{1}{2(|k|+iq)}\frac{K_\rho^+(k,q)}{K_\rho^*(k)}\right] \ , \tag{6.7}$$

$$\Omega^{(\mathrm{diff})}(k,q) = f_s(k)\Omega_s(k,q) \ , \qquad \Omega_s(k,q) \equiv \frac{k}{2\gamma'}\left[\frac{K_\Omega^+(k,q)}{K_\Omega^*(k)} - 1\right] \ . \tag{6.8}$$

The contribution of the diffuse source to the scattered flux is, according to Eq.(5.3),

$$\Phi_k^{(\mathrm{diff})} = -\Delta\Phi_k + \left[\gamma K_\rho^- S_\rho^- - K_\Omega^-\left(S_\Omega^- + S_\Omega^*\right)\right]_{q=-i|k|} \ . \tag{6.9}$$

We rewrite this as $f_s(k)\Phi_s(k)$, where

$$\Phi_s(k) \equiv \frac{1}{\pi} - \frac{\gamma}{4|k|\left[K_\rho^*(k)\right]^2} - \frac{|k|}{2\gamma'}\left\{1 - \frac{1}{\left[K_\Omega^*(k)\right]^2}\right\} \ .$$

In the long-wavelength limit, one can use the results of Appendix D to obtain the expansion

$$\Phi_s(k \to 0) = \frac{1}{\pi} - \frac{|k|}{\gamma} + \frac{k^2}{\gamma^2}\left(\frac{1}{\pi} + \frac{1}{2}\right) + O(|k|^3) \ . \tag{6.10}$$

The coefficient in the first term here can be understood if one considers a uniform diffuse source, i.e. the $k = 0$ limit. Such a source emits an equilibrium distribution and its effect can be compensated simply by shifting the chemical potential of the system by $\delta\mu = f_s$. Hence the upward distribution emitted by the source undergoes multiple collisions, and eventually arrives back at the wall as its mirror image. The respective flux can be found via an elementary calculation, by averaging $\sin\alpha$ over negative angles $-\pi < \alpha < 0$, which yields f_s/π. $f' \to f' + \delta\mu$, $f_s \to f_s + \delta\mu$. This causes In the opposite limit, $k \gg \gamma$, one may use Eq.(D7), writing $K^*_\rho(k) \approx 1$, $K^*_\Omega(k) \approx 1 + 2\gamma'/|k|$, so that $\Phi(k \to \infty) = -1/\pi$. The change in sign reflects that the excitation scattered back via a single collision event arrives as a hole rather than a particle.

VII. AN ISOTROPIC CURRENT EMITTER AT THE EDGE

Let us now analyse the contribution of a current source placed at the boundary. Assuming full isotropy, it is convenient to extend the source into the lower semispace: $J(\alpha) = 2I_0\delta(x)\delta(y)$. Since the source emits the flux $\Delta\Phi(k) = I_0$ downwards, the total current has to be doubled. (Treatment of a one-sided emitted is discussed in Appendix A.) The angular averaging in Eqs.(3.11) and (3.13) yields, with the help of Eq.(3.5):

$$\rho_{\rm dct}(k,q) = \frac{2I_0}{\sqrt{\gamma^2 + k^2 + q^2}} = \frac{\rho_{\rm dct}(k,q)}{K^-_\rho(k,q)} = \frac{2I_0}{\gamma}\left[1 - K_\rho(k,q)\right] \ , \qquad \Omega_{\rm dct}(k,q) = 0 \ . \tag{7.1}$$

The external current distribution is given by $\langle J_{\rm ext}(k,q)\rangle = I_0$. The functions $S^\pm_\rho(k,q)$ can be determined from

$$S^+_\rho(k,q) + S^-_\rho(k,q) = \frac{2I_0}{\gamma}\left[\frac{1}{K^-_\rho(k,q)} - \frac{1}{K^+_\rho(k,q)}\right] \ , \tag{7.2}$$

which suggests the straightforward decomposition

$$S^+_\rho(k,q) = \frac{2I_0}{\gamma}\left[1 - \frac{1}{K^+_\rho(k,q)}\right] \ , \qquad S^-_\rho(k,q) = \frac{2I_0}{\gamma}\left[\frac{1}{K^-_\rho(k,q)} - 1\right] \ . \tag{7.3}$$

(The constants are chosen to make $S^{\pm}_{\rho}(k,q)$ vanishing at $q \to \infty$.) Thus, the regular contribution to the density in Eq.(5.14) takes the form

$$\delta\rho_{\infty}(k,q) + \delta\rho_{\rm reg}(k,q) = \frac{\gamma' I_0}{|k|(|k|+iq)} \frac{K^{+}_{\rho}(k,q)}{K^{*}_{\rho}(k)} - \frac{2\gamma' I_0}{k^2+q^2} + \frac{2I_0}{\gamma}\left[K^{+}_{\rho}(k,q) + K_{\rho}(k,q) - 2\right] \ . \tag{7.4}$$

As before, we have subtracted the singular direct-flight contribution, which can be obtained by noticing that the particles isotropically emitted by the source propagate along straight lines and becoming extinct due to the decay rate γ. Hence their distribution is given by

$$f_{\rm dct}(\boldsymbol{r},\alpha) = \frac{2I_0}{|\boldsymbol{r}|} e^{-\gamma|\boldsymbol{r}|} \delta\left[\alpha - \arg(\boldsymbol{r})\right] \ , \tag{7.5}$$

where $\arg(\boldsymbol{r}) \equiv \tan^{-1}(y/x)$ is the polar angle. The resulting space-charge distribution is given by

$$\rho_{\rm dct}(\boldsymbol{r}) = \langle f_{\rm dct}(\boldsymbol{r},\alpha)\rangle = \frac{I_0}{\pi|\boldsymbol{r}|} e^{-\gamma|\boldsymbol{r}|} \ . \tag{7.6}$$

The vorticity equation is trivial, so that $S^{\pm}_{\Omega}(k,q) = 0$, and the vorticity in Eq. (5.23) includes only the regular part:

$$\Omega^{+}_{I}(k,q) = \delta\Omega_{I,\rm reg}(k,q) = I_0 \frac{K^{+}_{\Omega}(k,q)}{K^{*}_{\Omega}(k)} \tag{7.7}$$

The contribution to the downward flux can be found from $S^{-}_{\rho}(k,q)$ and $S^{-}_{\Omega}(k,q)$ similarly to Eq.(6.9):

$$\Phi^{(\rm edge)}_{k} = -I_0 + 2I_0\left[1 - \frac{1}{K^{*}_{\rho}(k)}\right] - \frac{\gamma\gamma' I_0}{2|k|^2\left[K^{*}_{\rho}(k)\right]^2} + \frac{I_0}{\left[K^{*}_{\Omega}(k)\right]^2} \ , \tag{7.8}$$

where the first term accounts for the extra injected flux $\Delta\Phi(k) = I_0$. We rewrite this in the form

$$\Phi^{(\rm edge)}(k) = I_0\Phi_I(k), \qquad \Phi_I(k) \equiv 1 - \frac{2}{K^{*}_{\rho}} - \frac{\gamma\gamma'}{2k^2\left[K^{*}_{\rho}(k)\right]^2} + \frac{1}{\left[K^{*}_{\Omega}(k)\right]^2} \ . \tag{7.9}$$

Let us discuss the behaviour of the flux given by Eq. (7.9). For purely viscous relaxation ($\gamma = \gamma'$), in the long-wavelength limit $k \to 0$, the expansions (D4) and (D5) yield:

$$\Phi_I(k\to 0) \approx \frac{2|k|}{\gamma}\left(\frac{1}{\pi} + \frac{1}{2} - \sqrt{2}\right) - \frac{2k^2}{\gamma^2}\left(\frac{1}{\pi} + \frac{1}{2} - \frac{1}{\sqrt{2}}\right)^2 + O(|k|^3) \ . \tag{7.10}$$

Note that the flux is suppressed at $k = 0$. Weak momentum relaxation, $\gamma'' \ll \gamma$, introduces an extra contribution, $\Phi_I(k=0) \approx \gamma''/\gamma$ which is responsible for the ohmic behaviour at

long distances. This can be explained as follows: a uniform source placed on the boundary produces a uniform upward-going flow which cannot be backscattered if momentum conservation is obeyed.

At large k, the single-collision contribution (D7) yields $\Phi_I(k \to \infty) = 2(\gamma'' - \gamma')/(\pi|k|)$. This short-distance behaviour describes backscattering of ballistic particles emitted by the source: the momentum-conserving collisions (γ') backscatter holes, while the ohmic relaxation (γ'') backscatter particles. The $1/|k|$ behaviour describes logarithmic divergence in the respective fluxes.

VIII. THE SELF-CONSISTENT SOLUTION FOR THE VICINITY-RESISTANCE GEOMETRY

We are now ready to derive self-consistent solution to current-injection problem by combining together the flow from the injector described in the previous section with the flow emitted by the diffuse wall described in Sec. VI. When the flux $I_0\Phi_I(k)$ of backscattered particles arrive at the diffuse wall at $y = 0$, a secondary diffuse source of intensity $f_s(k)$ is induced. Since the particles emitted by the secondary source are backscattered, an extra flux $\Phi_s(k)f_s(k)$ is produced, where $\Phi_s(k)$ is given by Eq.(6.9). Hence the intensity $f_s(k)$ of this source is to be determined self-consistently, via

$$\frac{f_s(k)}{\pi} = \Phi_I(k)I_0 + \Phi_s(k)f_s(k) \ , \tag{8.1}$$

which yields

$$f_s(k) = \frac{\pi\Phi_I(k)I_0}{1 - \pi\Phi_s(k)} \ . \tag{8.2}$$

(This relation is in fact true for an arbitary current source, if one replaces $\Phi_I(k)$ given by Eq. (7.9) by an appropriate expression.) Then, the carrier density is to be found as

$$\rho(k,q) = \rho_{\rm dct}(k,q) + \delta\rho_{I,\rm reg}(k,q) + f_s(k)\rho_s(k,q) \ , \tag{8.3}$$

where $\rho_s(k,q)$ and $\delta\rho_{I,\rm reg}(k,q)$ are given by Eq.(6.7) and (7.4) respectively. To perform the inverse Fourier transform with the factor $\exp(-iqy)$ with $y > 0$, it is convenient to shift the integration contour to the lower half-plane, as shown in Fig. 2. Keeping in mind that the electric potential in the bulk is proportional to the induced density, we write, in

dimensionless units:

$$\phi(\boldsymbol{r}) = \frac{I_0}{\pi|\boldsymbol{r}|}e^{-\gamma|\boldsymbol{r}|} + \int\limits_{-\infty}^{\infty} \frac{dke^{-ikx}}{2\pi} \oint\limits_{C+} \frac{dq}{2\pi} e^{-iqy} \left[\delta\rho_{I,\mathrm{reg}}(k,q) + f_s(k)\rho_s(k,q)\right] \ . \tag{8.4}$$

To determine the current distribution, we use vorticity $\Omega(k,q)$ which is a linear combination of the isotropic and diffuse flows found above:

$$\Omega(k,q) = \Omega_I(k,q) + f_s(k)\Omega_s(k,q) \ , \tag{8.5}$$

in which the individual contributions are defined in Eqs.(7.7) and (6.8). The current density can be found from Eqs.(3.18) with $D_{\boldsymbol{k}} = iI_0$ via the inverse Fourier transform. These relations can be also rewritten by introducing the stream function $\Psi(\boldsymbol{r})$ defined by $\boldsymbol{j} = \nabla\times\Psi$. The contribution of divergence $D_{\boldsymbol{k}}$ is simply an isotropic radial current emitted by the source. Such a flow is described by the multivalued stream function $\Psi_{\mathrm{rad}}(x,y) = I_0\pi^{-1}\arg(x,y)$. The charge-conserving contribution of $\Omega(k,q)$ can be rewritten in terms of the respective stream function $\Psi_\Omega(x,y)$ defined via $\boldsymbol{j} = \nabla\times\Psi$ if one defines the Fourier image $\Psi_\Omega(k,q)$ via $i\Omega(k,q) = \Psi(k,q)(k^2+q^2)$. Altogether, we find the stream function $\Psi(x,y)$ in the form

$$\Psi(x,y) = \frac{I_0}{\pi}\arg(x,y) + i\int\limits_{-\infty}^{\infty} \frac{dk\, e^{-ikx}}{2\pi} \oint\limits_{C+} \frac{dq}{2\pi} \frac{e^{-iqy}}{q^2+k^2} \left[\Omega_{I,\mathrm{reg}}(k,q) + f_s(k)\Omega_s(k,q)\right] \ . \tag{8.6}$$

Finally, the voltage $V(x)$ on the probe attached to the edge at position x is given by

$$V(x) = \int\limits_{-\infty}^{\infty} \frac{dk}{2\pi} f_s(k) e^{-ikx} \ . \tag{8.7}$$

We explain how these expressions can be recast into separate contirbutions of the singularities at $q = i|k|$ and $q = i\sqrt{k^2+\gamma^2}$ in Appendix F.

The solution that we have obtained describes the flow at all scales, from short scales $|\boldsymbol{r}| \ll \gamma^{-1}$ where the motion is purely ballistic to $|\boldsymbol{r}| \gg \gamma^{-1}$ where fluid mechanics is applicable. To extract these behaviours, we analyse the function $f_s(k)$ in the both limits. At large distances, $k \to 0$, substituting Eqs.(7.10) and (6.10) into Eq.(8.2) yields the expansion

$$\frac{f_{s,k}}{I_0} = \frac{\gamma''}{|k|} - C_0 + \frac{|k|}{\gamma} - C_2\frac{k^2}{\gamma^2} + O(|k|^3) \ , \tag{8.8}$$

with $C_0 = 2\sqrt{2} - 1 - 2/\pi \approx 1.192$, $C_2 \approx 0.7065$. (We omit a cumbersome expression for C_2.) Thus, finite ohmic relaxation rate always dominates at the longest distances, which

is expected. In a medium with conductivity σ, one expects the potential of a point source to be positive and log-divergent at large distances:

$$V(x) = \frac{I_0}{\pi\sigma} \log |\boldsymbol{r}| \ . \tag{8.9}$$

This matches our expression, if one applies Drude's formula for conductivity: $\sigma = ne^2\tau_p/m$, where n is the carrier density, and τ_p is momentum relaxation time. Since we are using dimensionless units (carrier mass $m^* = 1$, Fermi momentum $p_F = 1$, density of states $\nu = 1$), the carrier density is $n = \nu p_F^2/(2m^*) = 1/2$, and the Drude formula takes the form $\sigma^{-1} = 2\gamma''$, and the relation (8.9) is recovered if one Fourier transforms the term $\gamma''/|k|$, so that $V(\gamma'' x \gg 1) \approx (2\gamma''/\pi)\log(|x|)$.

Let us now focus upon the purely viscous case, $\gamma'' = 0$. The constant term $-C_0$ does not contribute to $V(x)$ far away, so we ignore it here and discuss its role later in this Section. The linear term $|k|/\gamma$ defines the behaviour of $V(x)$ in real space at large distances:

$$V(\gamma x \gg 1) \approx -\frac{I_0}{\pi\gamma x^2} \ , \tag{8.10}$$

which describes the viscous behaviour if one introduces the dynamic viscosity $\eta = 1/4l_{\rm ee}$ and uses the effective number density $n = 1/2$, as before. Indeed, the electric potential in e-fluid at large distances is expected[5] to behave as

$$\phi(x \gg l_{\rm ee}) \approx V(x) \approx -\frac{2}{\pi}\frac{I_0\eta}{(ne)^2}\frac{1}{x^2} \ . \tag{8.11}$$

if one assumes no-slip condition at the wall. The potential is negative as its gradient must compensate the drag force acting upon the stationary fluid at the no-slip edge from the moving fluid away from the edge. This comparison demonstrates that our solution faithfully reproduces the hydrodynamical limit in the purely viscous case. For weak momentum relaxation rate, $\gamma'' \ll \gamma$, the viscous term $|k|/\gamma$ dominates over the ohmic term $\gamma''/|k|$ at length scales $x \sim k^{-1} \ll (\gamma\gamma'')^{-1/2}$. The next-order term, $-C_2(k/\gamma)^2$, yields a contribution $\propto x^{-3}$, which represents the lowest-order correction to the viscous flow and can be partially attributed to the finite slip length $l_{\rm slip} = 2/\pi\gamma^{-1}$ (discussed in Sec. X), as well as other effects, e.g. the probe picking up higher harmonics of the carrier distribution.

Let us now discuss the short-distance behaviour. At large k, the expansion yields $f_s(k) \approx (\gamma'' - \gamma')/|k|$, which yields the negative log-divergent probe potential

$$V(x) = \frac{\gamma'' - \gamma'}{\pi} \log(\gamma|x|) \ . \tag{8.12}$$

which reproduces the flux due to backscattered holes analysed in[4] within the single-collision approximation. We note that the ballistic contribution probed by an edge contact remains negative for $\gamma'' < \gamma/2$, i.e. even in the regime where ohmic relaxation is strong, and one cannot observe fluidity in the bulk. We see therefore that the exact solution obtained here reproduces impeccably all important limiting behaviours, and hence provides a comprehensive description of fluidity onset in this geometry valid at all scales.

We have used this machinery to calculate the resulting distribution of charge and current densities numerically. The resulting flow pattern (i.e. the stream lines) is shown in Fig. 3. One can see that the character of the flow changes from isotropic at short distances, $|\boldsymbol{r}| < l_{\rm ee}$ to no-slip pattern at large distances. This indicates crossover to the viscous fluid regime of transport.

As was explained in Sec. II, the particle density $\rho(\boldsymbol{r})$ can be linked to the distribution of electric potential $\phi(\boldsymbol{r})$. The latter is shown as a pseudocolor plot in Fig. 3. At short distances, the potential exhibits $|\boldsymbol{r}|^{-1}$ singularity representing the space charge. At large distances, $|\boldsymbol{r}| > l_{\rm ee}$, this contribution is suppressed by collisions. The potential changes its sign at the two white diagonal lines and develops a quadrupolar pattern far away. In the fluid-mechanical analysis[5], this is explained as the effect of viscous drag.

In Fig. 4, we compare the electric potential $\phi(x, 0)$ at the edge with with the signal registered by an edge probe, $V_P(x) \propto f_s(x)$. The two quantities behave very differently at short distances, $|x| < l_{\rm ee}$ which indicates highly non-equilibrium distribution. Unlike electric potential, the probe potential is negative even at the shortest distances $|x| < l_{\rm ee}$ and does not exhibit space-charge behaviour. This indicates that the space-charge behaviour is due to charge carriers that are flying ballistically parallel to the edge and hence are not caught by the probe. The singularity $f_s(x) \propto \log(l_{\rm ee}/|x|)$ describes backscattering of holes into the probe[4], while the behaviour at large distances shown in the inset to Fig. 4 is described by fluid mechanics.

In practice, edge probe is fabricated at a fixed position x_P, while $l_{\rm ee}$ can be tuned by changing temperature or carrier density. Evolution of the probe potential with changing γ can be obtained from the data shown in Fig. 4 by employing an obvious scaling: $V_P(x) \propto \gamma f_s(\gamma x_P)$. The result is shown in Fig. 5. When $l_{\rm ee} < x_P$, one can observe a negative ballistic signal due to hole backscattering. The edge potential reaches the deep minimum at $\gamma x_P \approx 0.79$, which can be identified as fluidity onset. Indeed, when γ is increased further,

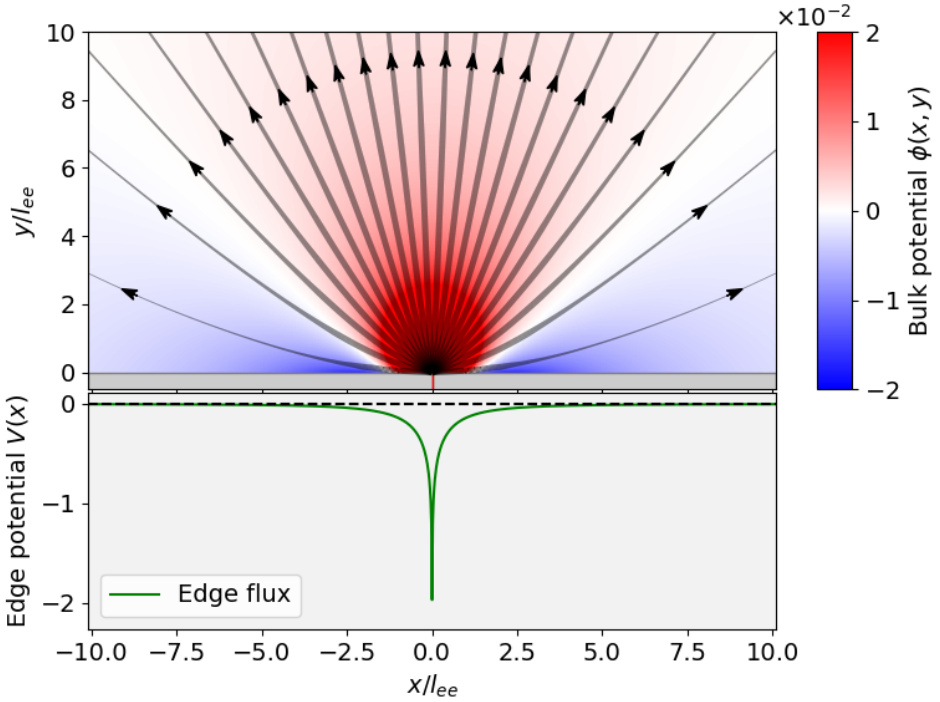

FIG. 3: Potential distribution $\phi(x, y)$ and stream lines for a flow generated by an isotropic current source attached to the edge. The distibution of edge voltage $V(x)$ is also shown in the bottom panel. Thicker lines indicate higher current density. At distances $|r| < l_{\rm ee}$ the flow is ballistic: the stream lines spread isotropically, and the bulk potential is positive due to the space charge. Fluidity is established at larger scales where the bulk potential distribution develops a quadrupolar sign-changing pattern[5], and the flow is redirected upward so that there is no slip at the wall. The edge potential $V(x)$, nevertheless, is negative at all scales.

the signal decreases and evolves into the viscous response.

The $k = 0$ limit, Eq. (8.8), also provides the solution to the contact-resistance problem. Let us replace a point source I_0 with a source equally distributed across the edge, $I_0(k) \approx \delta(k)$. Current emission results in an outgoing distribution $f'(\alpha) \propto 1/\sin\alpha$, which is partially backscattered into the current-emitting contact. The limit of $f_{s,k}$ at $k = 0$ gives the potential induced by near the contact and thus represents the contact resistance, $R_c \approx 1.192$. Restoring dimensionful units, one can show that this represents 1.192 of Sharvin's conductance, $h/(e^2 k_F W)$, where W is the width of the contact, and k_F is the Fermi momentum. The contact resistance, however, is not universal: it strongly depends upon the angular distribution of emitted particles, and one should repeat the analysis for a different choice of the source terms $\rho_{\rm dct}(k, q)$ and $\Omega_{\rm dct}(k, q)$ o describe contact resistance for a different distribution.

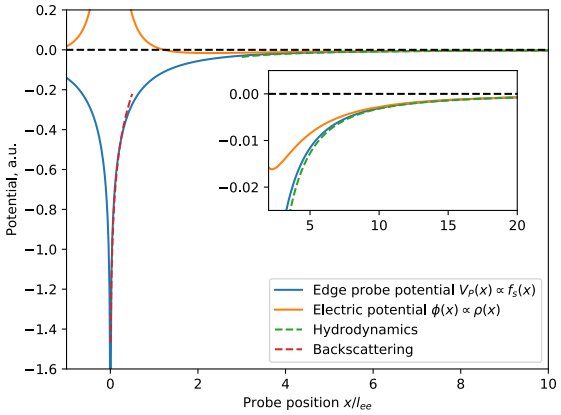

FIG. 4: The behaviour of both potentials near the source is shown as a function of probe position. At short distances, the negative signal in V_P is due to the holes backscattered into the edge[4]. Inset: long-distance behaviour. Local equilibrium is reached, the negative flux and density is due to the viscous drag[5].

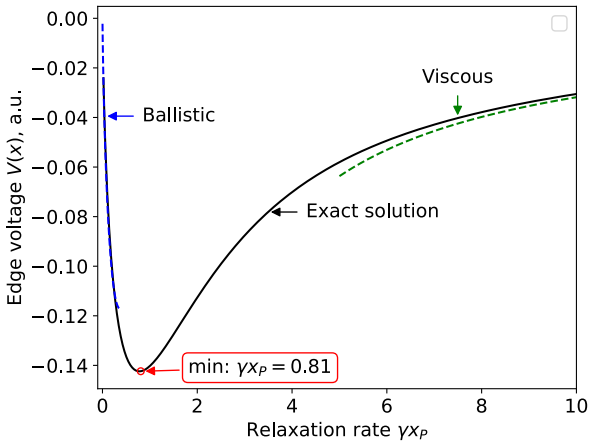

FIG. 5: Dependence of the edge voltage $V(x_P)$ upon the relaxation rate γ. The minimum of the potential separates the two regimes, ballistic and viscous, and hence marks the onset of fluidity.

One may also study a vicinity geometry with an anisotropic source. In particular, the diffuse solution presented in Sec. VI can be readily modified to describe a current source with sinusoidal directivity diagram, as shown in Appendix B. The comparison indicates that the viscous flow established at large scales is universal and is independent of the source directivity. The latter mostly affect phenomena at scales $|\boldsymbol{r}| \lesssim l_{\rm ee}$.

IX. CURRENT INJECTION IN THE INTERIOR

We can now consider a more difficult problem: an isotropic current source placed in the interior, at $y = h > 0$: $J(x, y, \alpha) = \delta(x)\delta(y - h)J_0$, which in the Fourier representation becomes $J_{\boldsymbol{k}}(\alpha) = e^{iqh}J_0$. The respective contributions to $\rho_{\rm dct}(k, q)$ and $\Omega_{\rm dct}(k, q)$ are obtained by translating the edge source considered previously, Eq.(7.1) to the point $y = h$, which is acccomplished by multiplying it by $\exp(iqh)$. The direct-flight density is given by

$$\rho^{(\rm int)}_{\rm dct} = \frac{J_0}{\gamma}\left[1 - K_\rho(k, q)\right] e^{iqh} \ , \tag{9.1}$$

with $K_\rho(k, q)$ defined via Eq.(3.9). The direct-flight contribution to the vorticity contribution vanishes: $\Omega^{(\rm int)}_{\rm direct} = 0$. Hence the solution for $\Omega^{\pm}_{\boldsymbol{k}}$ can be obtained immediately: they are proportional to $K^{\pm}_\Omega(k, q)$ so that the consistency condition (3.19) holds. Thus,

$$\Omega_{J,\boldsymbol{k}} = \Omega^+(k, q) = J^*_{\rm ext}(k)\frac{K^+_\Omega(k, q)}{K^*_\Omega(k)} = J_0 e^{-|k|h}\frac{K^+_\Omega(k, q)}{K^*_\Omega(k)} \ , \tag{9.2}$$

$$\Omega^-_{\boldsymbol{k}} = -J_0 e^{-|k|h}\frac{K^-_\Omega(k, q)}{K^*_\Omega(k)} \ . \tag{9.3}$$

The solution for the density, however, cannot be obtained in an explicit form. As outlined previously, one has to solve the Riemann-Hilbert problem

$$S^+_\rho(k, q) + S^-_\rho(k, q) = \frac{\rho_{\rm dct}(k, q)}{K^-_\rho(k, q)} = \frac{J_0}{\gamma}e^{iqh}\left[\frac{1}{K^-_\rho(k, q)} - \frac{1}{K^+_\rho(k, q)}\right] \ . \tag{9.4}$$

One may notice that the term $e^{iqh}/K^+_\rho(k, q)$ is complex-analytic at $\mathrm{Im}\, q > 0$ and hence does not contribute to $S^-_\rho(k, q)$. One may write, therefore,

$$S^-_\rho(k, q) = \frac{J_0}{\gamma}\oint\limits_{C_-}\frac{dq'}{2\pi i}\frac{e^{iq'h}}{(q - q' - i0)}\left[\frac{1}{K^-_\rho(k, q)} - 1\right] \ , \ . \tag{9.5}$$

where we subtracted unity to ensure convergence. The integration contour can be deformed into C_- shown in Fig. 2, as the factor e^{iqh} decays into the upper half-plane, which suppresses fast oscillations in the integrand. The downward flux $\Phi(k) = J_0\Phi_J(k)$ defined by Eq.(5.3) can be related to the value of $S^-_\rho(q = -i|k|)$ and $\Omega^-(k, q)$ above:

$$\Phi_J(l) \equiv \left\{-\frac{\gamma\gamma'}{2k^2\left[K^*_\rho(k)\right]^2} + \frac{1}{\left[K^*_\Omega(k)\right]^2}\right\} e^{-|k|h} + \frac{\gamma S^-_\rho(q = -i|k|)}{J_0 K^*_\rho(k)} \tag{9.6}$$

$$= \left\{-\frac{\gamma\gamma'}{2k^2\left[K^*_\rho(k)\right]^2} + \frac{1}{\left[K^*_\Omega(k)\right]^2}\right\} e^{-|k|h} - \frac{1}{K^*_\rho(k)}\oint\limits_{C_-}\frac{dq}{2\pi i}\frac{e^{iqh}}{q + i|k|}\left[\frac{1}{K^-_\rho(k, q)} - 1\right] \ .$$

Furthermore, one can rewrite the remaining integral in terms of the pole and the cut, similarly to Appendix F. The reside of $K_\rho^-(k,q)$ at $q=-i|k|$ is equal to $-\gamma^2/\left[|k|K_\rho^*(k)\right]$, cf. Eq.(F3) and its discontinuity across the cut is similar to Eq.(F4), which brings the flux to the form

$$\Phi_J(k)=\left\{\frac{\gamma\gamma''}{2k^2\left[K_\rho^*(k)\right]^2}+\frac{1}{\left[K_\Omega^*(k)\right]^2}\right\}e^{-|k|h}+\frac{\gamma}{K_\rho^*(k)}\int\limits_{\sqrt{k^2+\gamma^2}}^{\infty}\frac{ds}{\pi}\frac{e^{-hs}\sqrt{s^2-k^2-\gamma^2}}{(s+|k|)(s^2-k^2)K_\rho^+(is)}\ . \tag{9.7}$$

Once the flux $\Phi_J(k)$ is found, the secondary source on the boundary is to be determined self-consistently,

$$f_s(k)=\frac{\pi J_0\Phi_J(k)}{1-\pi\Phi_s(k)}\ , \tag{9.8}$$

cf Eq.(8.2). The induced density in the Fourier space can be obtained as before,

$$\rho(k,q)=\rho_{\rm dct}(k,q)+\delta\rho_J(k,q)+f_s(k)\rho_s(k,q) \tag{9.9}$$

with the source contribution $\delta\rho_J(k,q)$ defined by the general relations (5.13)–(5.15):

$$\begin{aligned}\delta\rho_J(k,q)=&-K_\rho^+(k,q)S_\rho^-(k,q)+\frac{\gamma' J_0e^{-|k|h}}{|k|(|k|+iq)}\frac{K_\rho^+(k,q)}{K_\rho^*(k)}\\&+\frac{J_0}{\gamma}e^{iqh}\left[K_\rho(k,q)+K_\rho^{-1}(k,q)-2\right]-\frac{2\gamma' J_0e^{iqh}}{k^2+q^2},\end{aligned} \tag{9.10}$$

However, evaluating this contribution in real space requires some care. The respective Fourier integral,

$$\int\limits_{-\infty}^{\infty}\frac{dq}{2\pi}e^{-iqy}\delta\rho_J(k,q) \tag{9.11}$$

involves oscillating contributions of two kinds: (i) the terms $\propto\exp(-iqy)$, and (ii) those that vary $\propto\exp\left[iq(h-y)\right]$. For the integrals of the first kind, one is allowed to pull the integration contour into the lower half-plane at all $y>0$, whereas for the terms $\propto\exp(iq(h-y))$ this is only allowed for $y>h$. This difficulty is resolved by noticing that the rest of the integrand is an even function of q, hence the integral in fact depends only upon $|y-h|$. Thus, one may recast $\delta\rho_J(x,y)$ into the form

$$\begin{aligned}\delta\rho_J(x,y)=\int\limits_{-\infty}^{\infty}\frac{dk}{2\pi}\,e^{-ikx}\oint\limits_{C_+}\frac{dq}{2\pi}\left\{e^{-iqy}\left[-K_\rho^+(k,q)S_\rho^-(k,q)+\frac{\gamma' J_0e^{-|k|h}}{|k|(|k|+iq)}\right]\right.\\\left.+\frac{J_0}{\gamma}\,e^{-iq|y-h|}\left[K_\rho(k,q)+K_\rho^{-1}(k,q)-2-\frac{2\gamma\gamma'}{k^2+q^2}\right]\right\}\ ,\end{aligned} \tag{9.12}$$

with $S_\rho^-(k,q)$ defined by Eq.(9.5). The term $\rho_{\rm dct}(x,y)$ can be derived similarly to Eq. (7.6):

$$\rho_{\rm dct}(\boldsymbol{r}) = \frac{I_0}{2\pi|\boldsymbol{r}|} e^{-\gamma|\boldsymbol{r}|} \ , \tag{9.13}$$

while the diffuse scattering contribution retains the same form as in Eq.(8.4), (6.7) but with the edge flux $f_s(k)$ given by Eq.(9.8). The stream function can be also found as before, with the appropriate modifications in the source term:

$$\Psi(x,y) = \frac{I_0}{2\pi} \arg(x, y-h) + i \int\limits_{-\infty}^{\infty} \frac{dk\, e^{-ikx}}{2\pi} \oint\limits_{C+} \frac{dq}{2\pi} \frac{e^{-iqy}}{q^2+k^2} \left[\Omega_J(k,q) + f_s(k)\Omega_s(k,q)\right] \ . \tag{9.14}$$

Here $\Omega_J(k,q)$ is defined by Eq.(9.2), while $\Omega_s(k,q)$ is again given by Eq.(6.8).

As in the previous section, the solution can be employed to obtain current and potential patterns. Stream function and potential distribution for $h/l_{\rm ee} = 3$ are shown in Fig. 6. The downward flow emitted by the source is transformed when it hits the edge. This results in an extra broad component of the potential distribution. One can see that at sufficiently large distances ($|\boldsymbol{r}| > h$) the flow is similar to the one emitted by a point source on the edge. However, the sign change in the edge potential occurs at $x \approx h$ instead of $l_{\rm ee}$. Evolution of the probe signal with ee relaxation rate is shown in Fig. 7. In close proximity to the source, the flux is always positive, fading away into the viscous regime as $\propto l_{\rm ee}$. Further away, it changes the sign and exhibits a weaker minimum at the onset of fluidity, $\gamma h \approx 1$.

X. MOMENTUM SOURCE IN THE INTERIOR (THE STOKESLET)

We now consider the effect of a concentrated force $\boldsymbol{F} = (F_x, F_y)$ applied to the fluid at some interior point $(0,h)$. This can be described by the source term

$$J^{(F)}(x,y,\alpha) = 2(F_x \cos\alpha + F_y \sin\alpha)\delta(x)\delta(y-h) \ , \tag{10.1}$$

so that the rate at which momentum is injected into the fluid is $\langle J(x,y)\boldsymbol{v}\rangle = \boldsymbol{F}$. In fluid mechanics, this quantity is known as the Stokeslet. In an infinite space, the pressure induced by the source at the origin is given only by the longitudinal component of the force, $p(\boldsymbol{r}) = \boldsymbol{F}\cdot\widehat{\boldsymbol{r}}/(2\pi|\boldsymbol{r}|)$, and is independent of viscosity. But in a restricted geometry the pressure becomes coupled to the vorticity and acquires a long-range component that depends upon the boundary conditions. It is therefore interesting to derive the Stokeslet near the fluidity onset.

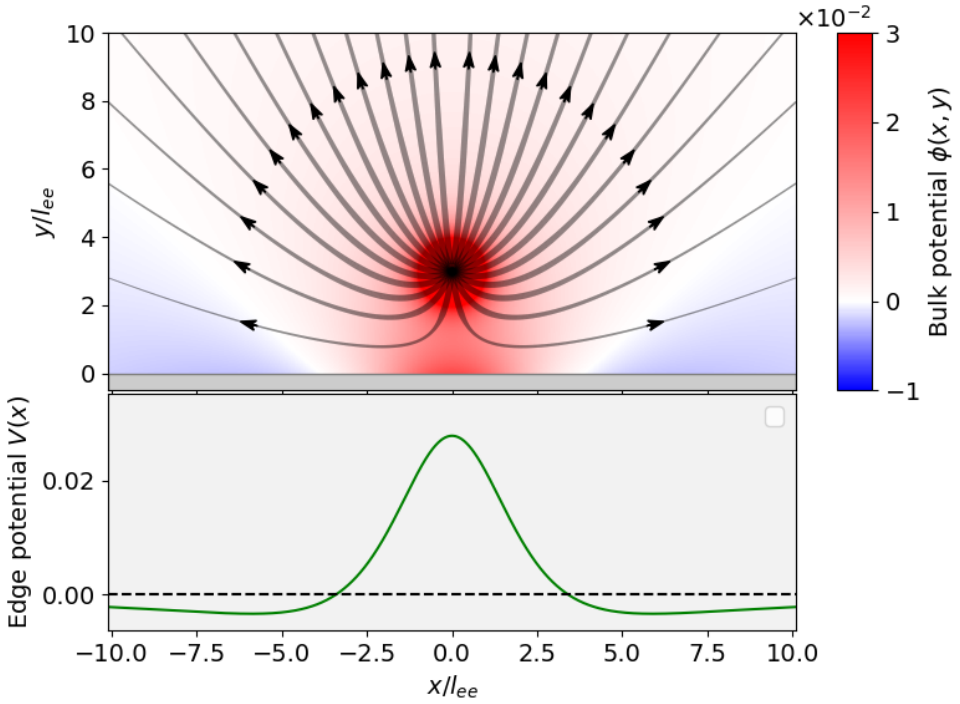

FIG. 6: Electric potential distribution induced by a current injector placed $3l_{\rm ee}$ away from the edge.

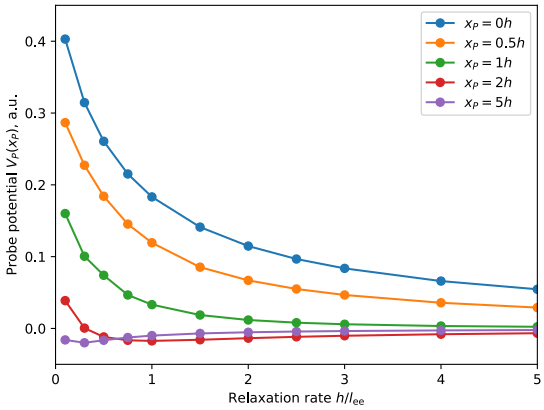

FIG. 7: Evolution of edge probe signal with increasing relaxation rate γ.

The respective direct-flight contributions are computed with the help of Eq. (3.5), which yields

$$\rho^{(F)}_{\rm dct}(k,q) = \frac{2i\boldsymbol{k}\cdot\boldsymbol{F}}{k^2+q^2}K_\rho(k,q)e^{iqh}\ , \qquad \Omega^{(F)}_{\rm dct} = \frac{\boldsymbol{k}\times\boldsymbol{F}}{\gamma'}\left[1-K_\Omega(k,q)\right]e^{iqh}\ , \tag{10.2}$$

with $\boldsymbol{k}\cdot\boldsymbol{F} = kF_x + qF_y$, $\boldsymbol{k}\times\boldsymbol{F} = kF_y - qF_x$. The source does not inject particles, so that $D^+(k,q) = i\langle J\rangle = 0$. Comparing this with the previous problem, one can notice the duality through which the density and vorticity interchange their roles. As before, to

determine the induced density, one has to decompose

$$\frac{\rho^{(}_{\rm dct}F)(k,q)}{K_\rho^-(k,q)} = \frac{2i\boldsymbol{k}\cdot\boldsymbol{F}}{k^2+q^2}\frac{e^{iqh}}{K_\rho^+(k,q)} \ . \tag{10.3}$$

The decomposition is achieved by eliminating the pole at $q = i|k|$, which yields

$$\rho_F(k,q) \equiv \rho^+(k,q) = \frac{2i\boldsymbol{k}\cdot\boldsymbol{F}}{k^2+q^2}e^{iqh} - \frac{i\,\mathrm{sgn}\,kF_x - F_y}{|k|+iq}\frac{K_\rho^+(k,q)}{K_\rho^*(k)}e^{-|k|h} \ , \tag{10.4}$$

$$\rho^-(k,q) = \frac{i\,\mathrm{sgn}\,kF_x - F_y}{|k|+iq}\frac{K_\rho^-(k,q)}{K_\rho^*(k)}e^{-|k|h} \ . \tag{10.5}$$

To determine the vorticity, one has to solve the Riemann-Hilbert problem

$$S_\Omega^+(k,q) + S_\Omega^-(k,q) = \frac{kF_y - qF_x}{\gamma'}e^{iqh}\left[\frac{1}{K_\Omega^-(k,q)} - \frac{1}{K_\Omega^+(k,q)}\right] \ , \tag{10.6}$$

similar to Eq. (9.4). The solution is again given by the Cauchy integral (5.26), in which one can ignore the contribution $\propto 1/K_\Omega^+(k,q)$. Following the discussion in Sec. V, we incorporate the constant $S_\Omega^*(k,i|k|)$ into $S_\Omega^-(k,q)$ and write

$$\tilde{S}_\Omega(k,q) = \oint\limits_{C_-}\frac{dq'}{2\pi i}\frac{(i|k|-q)e^{iq'h}}{(q-q'-i0)(i|k|-q'-i0)}\frac{kF_y - q'F_x}{\gamma'}\left[\frac{1}{K_\Omega^-(k,q')} - 1\right] \ , \tag{10.7}$$

in which we again deform the integration contour into C_- shown in Fig. 2(c). The vorticity is then given by the singular direct-flight contribution and a smoother background:

$$\Omega^+(k,q) = \Omega_{\rm dct}(k,q) + \delta\Omega_{F,\rm reg}(k,q) \ , \tag{10.8}$$

with

$$\delta\Omega_{F,\rm reg}(k,q) = -K_\Omega^+(k,q)\tilde{S}_\Omega(k,q) + \frac{\boldsymbol{k}\times\boldsymbol{F}}{\gamma'}\left[K_\Omega(k,q) + K_\Omega^{-1}(k,q) - 2\right]e^{iqh} \ . \tag{10.9}$$

Evaluating the downward flux $\Phi_F(k)$ from Eq.(5.3), with $\Omega^-(k,q) = -K_\Omega\tilde{S}_\Omega(k,q)$ and $\rho^-(k,q)$ given by Eq.(10.4), we write

$$\Phi_F(k) = \frac{\gamma}{2|k|}\frac{F^*(k)}{\left[K_\rho^*(k)\right]^2}e^{-|k|h} - \frac{\mathrm{sgn}\,k}{K_\Omega^*(k)}\tilde{S}_\Omega(k,-i|k|) \ , \tag{10.10}$$

with $F^*(k) \equiv iF_x\,\mathrm{sgn}\,k - F_y$. For $q = -i|k|$ the Cauchy integral simplifies to

$$\Phi_F(k) = (iF_x\,\mathrm{sgn}\,k - F_y)e^{-|k|h}\left[\frac{\gamma}{2|k|\left[K_\rho^*(k)\right]^2} - \frac{|k|}{\gamma'\left[K_\Omega^*(k)\right]^2}\right] - \frac{|k|}{\gamma'}\oint\limits_{C_-}\frac{dq'}{\pi}\frac{e^{iq'h}}{q'^2+k^2}\frac{kF_y - q'F_x}{K_\Omega^-(k,q')} \ , \tag{10.11}$$

where the remaining contour integral can be further transformed into the sum of the contributions from the pole and the cut which we do not attempt here. As before, $f_s(k)$ is obtained from flux conservation condition, $f_s(k) = \pi\Phi_F(k)/[1 - \pi\Phi_s(k)]$, and the full density and vorticity are given by

$$\rho(k,q) = \rho_F(k,q) + f_s(k)\rho_s(k,q) \ , \tag{10.12}$$

$$\Omega(k,q) = \Omega_{\rm dct}(k,q) + \delta\Omega_F(k,q) + f_s(k)\Omega_s(k,q) \ , \tag{10.13}$$

with $\rho_F(k,q)$ defined by Eq.(10.4), $\rho_s(k,q)$ by Eq.(6.7), $\delta\Omega_F(k,q)$ by Eq.(10.9), and $\Omega_s(k,q)$ by Eq.(6.8). These can be used to determine the potential $\phi(\boldsymbol{r})$ and the stream function $\Psi(\boldsymbol{r})$. As in the previous Section, for $y < h$ one has to pay attention to the oscillating contributions $\propto \exp[iq(h-y)]$, e.g. continuing these from $y > h$. In the potential, the integral of the term proportional to $\boldsymbol{k}\cdot\boldsymbol{F}$ gives the Stokeslet in an infinite space, while the rest gives the regular correction due to the scattered particles:

$$\begin{aligned}\phi(\boldsymbol{r}) = \frac{1}{\pi}\frac{xF_x + (y-h)F_y}{x^2+(y-h)^2} \\ + \int\limits_{-\infty}^{\infty}\frac{dk}{2\pi}\,e^{-ikx}\oint\limits_{C_+}\frac{dq}{2\pi}e^{-iqy}\left[-\frac{i\,\mathrm{sgn}\,kF_x - F_y}{|k|+iq}\frac{K_\rho^+(k,q)}{K_\rho^*(k)}e^{-|k|h} + f_s(k)\rho_s(k)\right] \ .\end{aligned} \tag{10.14}$$

The stream function is given by

$$\begin{aligned}\Psi(\boldsymbol{r}) = \Psi_{\rm dct}(\boldsymbol{r}) + \int\limits_{-\infty}^{\infty}\frac{dk}{2\pi}\,e^{-ikx}\oint\limits_{C_+}\frac{dq}{2\pi}\,\frac{1}{q^2+k^2}\left\{\left[-K_\Omega^+(k,q)\tilde{S}_\Omega(k,q) + f_s(k)\rho_s(k)\right]e^{iqy}\right. \\ \left. + \,\frac{K_\Omega(k,q) + K_\Omega^{-1}(k,q) - 2}{\gamma'}\left[kF_y - qF_x\,\mathrm{sgn}(y-h)\right]e^{iq|y-h|}\right\} \ .\end{aligned} \tag{10.15}$$

The direct-flight contribution to the stream function can be found by integrating the respective current distribution

$$\boldsymbol{j}_{\rm dct}(\boldsymbol{r}) = \nabla\times\Psi_{\rm dct}(\boldsymbol{r}) = \frac{2\boldsymbol{F}\cdot(\boldsymbol{r}-\boldsymbol{r}_h)\,(\boldsymbol{r}-\boldsymbol{r}_h)}{|\boldsymbol{r}-\boldsymbol{r}_h|^3}e^{-\gamma|\boldsymbol{r}-\boldsymbol{r}_h|} \ , \tag{10.16}$$

where $\boldsymbol{r}_h = (0,h)$ is the position of the source.

The stream pattern and the potential induced by a point momentum source acting in the x-direction (parallel to the edge) are shown in Fig. 8 for $h = 0.5l_{\rm ee}$. The flow and the potential for a source acting along the y axis are showin in Fig.9. The two stream patterns

are strongly affected by the edge. This can be seen e.g. by noting that 8 cannot be obtained from Fig.9 via a 90° rotation, as one would expect in an infinite system. Paradoxically, this is true even when the source is moved away from the edge as can be seen in Fig. 10 where the source is moved further away from the edge, $h = 5l_{\rm ee}$. To resolve this paradox, one can first calculate the Stokeslet in an infinite space starting either from the Stokes equation, or from the Boltzmann equation and taking the limit $|\boldsymbol{k}| \ll \gamma$. This way, one can identify a logarithmic infrared divergence in the current distribution. This divergence indicates that in two dimensions the Stokeslet cannot be properly defined without considering the effect of boundary conditions irrespective of the distance to the edge. The boundary condition regularises the log-divergence differently for two different orientation of the momentum source, and this is seen as the difference between Figs. 8 and 9.

This physics, however, is not seen in the edge probe potentials shown in Figs. 11 and 12 respectively for different values of electron-electron mean-free path $l_{\rm ee}$. One can see that the edge potential dependence on $l_{\rm ee}$ is very weak. To explain this, note that the Stokeslet in an infinite space is characterised by pressure response by $p(\boldsymbol{r}) = \boldsymbol{F} \cdot \boldsymbol{r} r^2$, where $\boldsymbol{F}$ is the force applied at the origin. This relation holds irrespective of the relationship between $|\boldsymbol{r}|$ and $l_{\rm ee}$. Apparently, edge potentials shown in Figs. 11 and 12 receive the dominant contribution from this longitudinal mode.

Experimentally, point momentum source can be realised in scanning microscopy experiments in which the scanning gate depletes the system and thus blocks the passage of current[8]. A simple model for this is a perturbation of a flow by a pointlike scatterer. Introducing the scatterer to the right-hand side of Boltzmann's equation, one can see that it effectively acts as a source of momentum and higher angular harmonics of the distribution function. (Emission of the density harmonic is suppressed by particle number conservation.) At large distances, the effect of the scatterer is dominated by the lowest harmonic, i.e. by x- and y-components of momentum.

Our solution can be also employed to extract the slip length λ. To this end, consider the limit of uniform flow, $k = 0$, in which the source of x-momentum is distributed over the interior, e.g. $F_x(y) = F_0 \exp(-\delta y)$, where $\delta \ll y$. Such a force induces a Poiseuille-like flow in which the role of the channel width W is played by δ^{-1}. The equation for vorticity,

$$K_\Omega(0,q)\Omega_q^+ + \Omega_q^- = -\frac{qF_0}{2\gamma(\delta - iq)}\left[1 - K_\Omega(0,q)\right] \ , \tag{10.17}$$

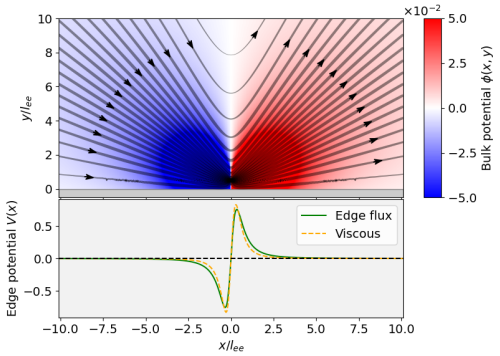

FIG. 8: Stream lines and the potential distribution for a flow induced by a point momentum source acting parallel to the wall and placed at $(0, 0.5l_{\mathrm{ee}})$.

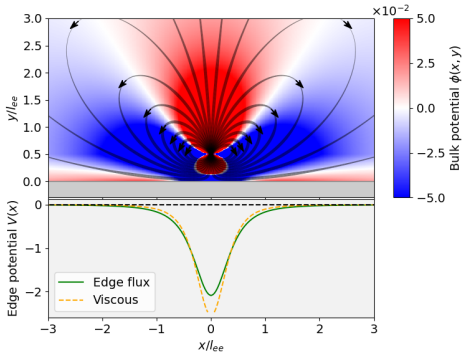

FIG. 9: Stream lines and the potential distributoin for a flow induced by a point momentum source acting perpendicular to the wall and placed at $(0, 0.5l_{\mathrm{ee}})$.

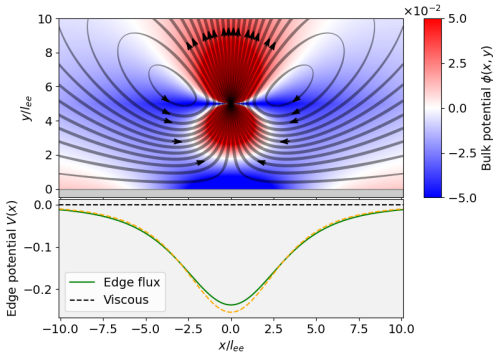

FIG. 10: Stream lines and the potential distributoin for a flow induced by a point momentum source acting perpendicular to the wall and placed at $(0, 5l_{\mathrm{ee}})$.

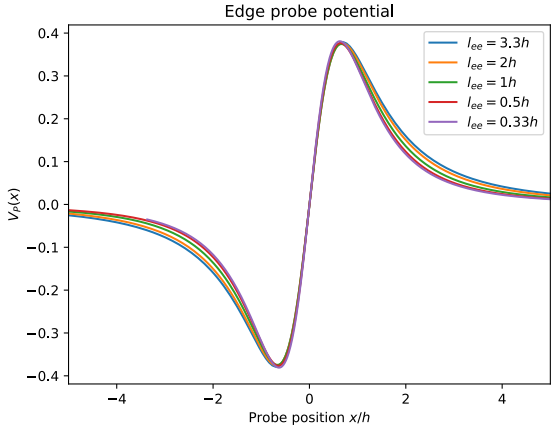

FIG. 11: The potential induced at the edge by a flow shown in Fig. 8.

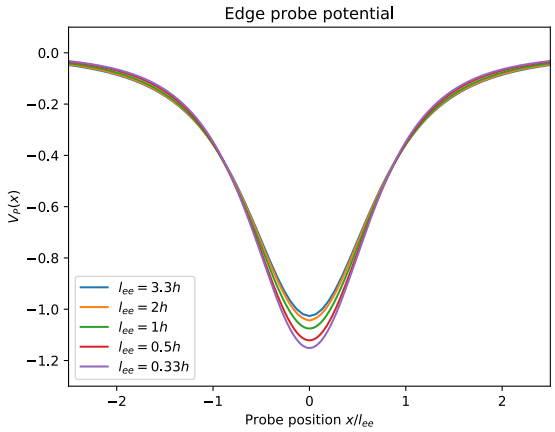

FIG. 12: The potential induced at the edge by a flow shown in Fig. 9.

is readily solved by dividing both sides by $K_\Omega^-(0,q)$, separating the pole at $q = -i\delta$ from Ω^-, and using the consistency condition $\Omega^+(0,0) = 0$. This yields

$$\Omega_q^+ = \frac{F_0}{2\gamma}\frac{q}{\delta - iq}\left[1 - \frac{K_\Omega^+(0,q)}{K_\Omega^-(0,-i\delta)}\right] . \tag{10.18}$$

By definition, the slip length is obtained by extrapolating current profile at $y \gg \gamma^{-1}$ to $y = 0$. Hence we consider the current density $j_x(y)$ at $\gamma^{-1} \ll y \ll \delta^{-1}$, i.e. at $\delta \ll q \ll \gamma$. Employing the results of Appendix E

$$K_\Omega^+(0, q \ll \gamma) \approx \frac{2\gamma}{-iq} + \frac{4}{\pi} , \tag{10.19}$$

one finds the two leading terms:

$$j_x(q) = -\frac{\Omega_q^+}{q} = -\frac{2\gamma F_0}{q^2\delta} + \frac{4}{(-iq)\pi\delta} . \tag{10.20}$$

In real space, the first term represents a uniform velocity shear near the edge, $j_x^{(1)}(y) = 2\gamma F_0 \delta^{-1} y$, while the second term adds a constant offset: $j_x^{(2)} = 4/\pi\delta^{-1}$. The slip length is therefore given by $\lambda = 2/(\pi\gamma) \approx 0.64\gamma^{-1}$.

It is interesting to compare this result with the result for $f_s(k)$ due to a point source. Solving hydrodynamical equations with a finite slip length λ, one finds for Fourier components of pressure at the edge: $p_k \propto |k|(1+\lambda|k|)/(1+2\lambda|k|) \approx |k| - \lambda|k|^2$. Naively, one should expect the density at the edge $f_s(k)$ to be proportional to pressure. Using our result for λ, one finds the quadratic term to be $-0.64|k|^2/\gamma$. This is close to our previous result, Eq.(8.8), in which the relevant coefficient is -0.707. The difference is due to the variation of the density near the edge at distances $y \sim \gamma^{-1}$.

XI. CONCLUSION

Mention Landauer's dipoles

Analytical treatment of fluidity onset in this article can be employed to provide detailed answers to many questions, to make connections with experiments, and perhaps to develop approximate schemes for many interesting setups which are not covered here. For example, one can also incorporate Drude momentum relaxation into the Wiener-Hopf approach by modifying the kernels $K_\rho(k,q)$ and $K_\Omega(k,q)$. Another interesting open questions is whether it is possible to incorporate (weak) external magnetic field into the formalism, which is important for a number of interesting measurements.

The solution, besides being fully quantitative, provides some interesting insights. For example, the ability to represent the solution in terms of pole and cut contribution describes a separation between degrees of freedom which can be helpful for qualitative analysis.

to be continued.

Appendix A: Treating one-sided boundary sources

In this appendix, we show how one can treat boundary sources, i.e., an isotropic emitter and a Lambertian diffuse source, without extending them to the lower semispace.

Let us begin with the emitter described by the source term $J^{\text{edge}}(x,y,\alpha) = 2I_0\delta(x)\delta(y)\Theta(\alpha)$, where I_0 is the total current injected by the source. In the Fourier representation, this be-

comes $J_{\boldsymbol{k}}(\alpha) = I_0\Theta(\alpha)/\pi$. The respective direct-flight contribution to the density reads

$$\rho^{(\mathrm{edge})}_{\mathrm{dct}}(k,q) = \int\limits_0^\pi \frac{d\alpha}{2\pi}\frac{J_{\boldsymbol{k}}(\alpha)}{\gamma - i\boldsymbol{k}\cdot\boldsymbol{v}} = 2I_0F_m(k,q)\ . \tag{A1}$$

The quantity

$$F_m(k,q) \equiv \int\limits_0^\pi \frac{d\alpha}{2\pi}\frac{1}{\gamma - ik\cos\alpha - iq\sin\alpha} \tag{A2}$$

represents the "master integral" through which we shall express all other contributions of "one-sided" sources. A straightforward calculation (e.g. by changing the integration variable to $z = e^{i\alpha}$) yields

$$F_m(k,q) = \frac{1}{2\sqrt{k^2+q^2+\gamma^2}}\left[1 + \frac{2i}{\pi}\log\frac{q+\sqrt{q^2+k^2+\gamma^2}}{\sqrt{k^2+\gamma^2}}\right] \tag{A3}$$

(the logarithm in the brackets can be also written as $\sinh^{-1}(q/\sqrt{k^2+\gamma^2})$). By definition, this function is complex-analytic at $\mathrm{Im}\, q > 0$, as all poles in the integrand are at $\mathrm{Im}\, q < 0$ for upward-going particles. The function $F_m(k,q)$ satisfies the identity

$$F_m(k,q) + F_m(k,-q) = \frac{1 - K_\rho(k,q)}{\gamma}\ , \tag{A4}$$

in which the right-hand side describes a fully isotropic current source, cf. Eq.(7.1), while the two terms on the left-hand side describe upward-going and downward-going particles. The function $F_m(k,-q)$ is complex-analytic in the lower half-plane. The direct-flight contribution to the vorticity is also straightforward, and one arrives at a q-indepdendent expression:

$$\Omega^{(\mathrm{edge})}_{\mathrm{dct}}(k,q) = \int\limits_0^\pi \frac{d\alpha}{2\pi}\frac{J_{\boldsymbol{k}}(\alpha)(\boldsymbol{k}\times\boldsymbol{v})}{\gamma - i\boldsymbol{k}\cdot\boldsymbol{v}} = \frac{2I_0}{\pi}\tan^{-1}\frac{k}{\gamma}\ . \tag{A5}$$

Now we can solve the Wiener-Hopf equations with these sources. To decompose the source in the density equation into $S^\pm_\rho(k,q)$, we apply the identity (A4):

$$S^+_\rho(k,q) + S^-_\rho(k,q) = \frac{2I_0F_m(k,q)}{K^-_\rho(k,q)} = \frac{2I_0}{\gamma}\left[-\frac{\gamma F_m(k,-q)}{K^-_\rho(k,q)} + \frac{1}{K^-_\rho(k,q)} - \frac{1}{K^+_\rho(k,q)}\right]\ . \tag{A6}$$

Since the function $F_m(k,-q)$ is analytic at $\mathrm{Im}\, q < 0$, the first two terms can be grouped into $S^-_\rho(k,q)$. Hence we find the solution decaying at $q\to\infty$:

$$S^-_\rho(k,q) = \frac{2I_0}{\gamma}\left[-\frac{\gamma F_m(k,-q)}{K^-_\rho(k,q)} + \frac{1}{K^-_\rho(k,q)} - 1\right]\ , \tag{A7}$$

while $S_\rho^+(k,q)$ is the same as in Eq. (7.3), so that only the density $\rho^-(k,q)$ is changed by $\Delta\rho^-(k,q) = -I_0 F_m(k,-q)$. Since the vorticity contribution given by Eq.(A5) is q-independent, we can also absorb this constant by shifting $\Omega^-(k,q)$ without changing $\Omega^+(k,q)$. Thus, the only change occurs in the expression for the downward-going flux, see Eq. (5.3):

$$\Delta\Phi(k) = \gamma\Delta\rho^-(k,-i|k|) - \operatorname{sgn} k\,\Omega^-(k,-i|k|) = I_0\left[-F_m(k,i|k|) + \frac{2}{\pi}\tan^{-1}\frac{|k|}{\gamma}\right] . \quad \text{(A8)}$$

With the help of Eq. (A3), this simplifies to $\Delta\Phi(k) = -I_0/\gamma$, which coincides with the extra flux employed in Eqs.(7.8) and (7.9).

Let us now perform the same analysis for a diffuse source $J(x,y,\alpha) = f_s(x)\sin\alpha\delta(y)$ restricted to upward movers. The source in the density equation

$$\rho_{\rm dct}^{\rm (diff)}(k,q) = f_s(k)F_\rho(k,q) , \quad \text{(A9)}$$

can be expressed via the master integral:

$$F_\rho(k,q) \equiv \int_0^\pi \frac{\sin\alpha}{\gamma - ik\cos\alpha - iq\sin\alpha}\frac{d\alpha}{2\pi} = \frac{1}{k^2+q^2}\left[\frac{k}{\pi}\tan^{-1}\frac{k}{\gamma} + \frac{iq}{2} - i\gamma q F_m(k,q)\right] . \quad \text{(A10)}$$

It obeys an identity similar to Eq. (A4):

$$F_\rho(k,q) - F_\rho(k,-q) = \frac{iq}{q^2+k^2}K_\rho(k,q) , \quad \text{(A11)}$$

where again the right-hand side represents a source extended to the whole unit circle, cf. Eq. (6.10), which is decomposed into upward- and downward movers. The function $F_\rho(k,q)$ is analytic in the upper half-plane, while the function $F_\rho(k,-q)$ is analytic in the lower half-plane. The respective vorticity contribution $\Omega_{\rm dct}^{\rm (diff)}(k,q) = f_s(k)F_\Omega(k,q)$, is again expressed via the master integral:

$$\begin{aligned} F_\Omega(k,q) &\equiv \int_0^\pi \frac{\sin\alpha(k\sin\alpha - q\cos\alpha)}{\gamma - ik\cos\alpha - iq\sin\alpha}\frac{d\alpha}{2\pi} \quad \text{(A12)} \\ &= k\left(1 + \frac{\gamma^2}{k^2+q^2}\right)F_m(k,q) - \frac{1}{2}\frac{\gamma k}{k^2+q^2} - \frac{i}{\pi}\frac{\gamma q}{k^2+q^2}\tan^{-1}\frac{k}{\gamma} . \end{aligned}$$

The function $F_\Omega(k,q)$ obeys the identity

$$F_\Omega(k,q) + F_\Omega(k,-q) = \frac{k}{2\gamma'}\left[1 - K_\Omega(k,q)\right] , \quad \text{(A13)}$$

which has the same interpretation as Eqs.(A4) and (A11), with the right-hand side matching Eq.(6.10). The Wiener-Hopf equations are solved in the same manner as before. The function $\rho^-(k,q)$ acquires an extra contribution $\Delta\rho^-(k,q) = f_s(k)F_\rho(k,-q)$, while the function $\rho^+(k,q)$ is again determined by Eq. (6.7). Similarly, $\Omega^+(k,q)$ remains the same as in Eq.(6.8), while $\Omega^-(k,q)$ is shifted by $\Delta\Omega^-(k,q) = -f_s(k)F_\Omega(k,-q)$. The respective change in flux is given by

$$\Delta\Phi(k) = f_s(k)\left[F_\rho(k,i|k|) + \operatorname{sgn} k F_\Omega(k,i|k|)\right] \ . \tag{A14}$$

This simplifies to $f_s(k)/\pi$ with the help of Eqs.(A10) and(A12).

Appendix B: A source with sinusoidal directivity

In our analysis in Sec. VI, we have treated the Lambertian source as a secondary source that does not contribute to the total injected current $\langle J_{\rm ext}(k,q)$. One could instead consider a current source $I_s(k)$ with sinusoidal directivity $J(x,y,\alpha) = \pi I_s \sin\alpha\delta(x)\delta(y)$, so that $f_s(k) = \pi I_s(k)$. This would require some alterations in expressions for $\rho_s^+(k,q)$, $\Omega_s(k,q)$ and $\Phi_s(k)$. Following the general solution (5.8), we modify Eq.(6.7) as follows:

$$\rho^{(\rm sin)}(k,q) = I_s(k)\tilde\rho_s(k,q) \ , \qquad \tilde\rho_s(k,q) \equiv \frac{\pi i q - 2\gamma'}{k^2+q^2} + \frac{\pi|k| + 2\gamma'}{2|k|(|k|+iq)}\frac{K_\rho^+(k,q)}{K_\rho^*(k)} \ . \tag{B1}$$

Eq.(6.8) also acquires an extra contribution to satisfy Eq.(3.19):

$$\Omega^{(\rm sin)}(k,q) = I_s(k)\tilde\Omega_s(k) \ , \qquad \tilde\Omega_s(k,q) = \operatorname{sgn} k\left[1 + \frac{\pi|k|}{2\gamma'}\right]\frac{K_\Omega^+(k,q)}{K_\Omega^*(k)} - \frac{\pi k}{2\gamma'} \ . \tag{B2}$$

The downward flux now takes the form $\Phi^{(\rm sin)}(k) = \tilde\Phi_s(k)I_s(k)$, with

$$\tilde\Phi_s(k) \equiv 1 - \left\{\frac{\pi}{2} + \frac{\gamma'}{|k|}\right\}\left\{\frac{\gamma}{2|k|\left[K_\rho(k)^*\right]^2} - \frac{|k|}{\gamma'\left[K_\Omega^*(k)\right]^2}\right\} - \frac{\pi|k|}{2\gamma'} \ . \tag{B3}$$

Its expansion at $|k| \ll \gamma$ for $\gamma' = \gamma$ is given by

$$\tilde\Phi_s(k) = -\tilde C_1\frac{|k|}{\gamma} + \tilde C_2\frac{k^2}{\gamma^2} + O(|k|^3) \ , \qquad \tilde C_1 = \pi - 1 - \frac{2}{\pi} \approx 1.5049 \ , \qquad \tilde C_2 \approx 2.2315 \ . \tag{B4}$$

A self-consistent solution can be obtained similarly to Sec. VIII, with the secondary source given by $f_s(k) = \pi\tilde\Phi_s(k)/[1 - \pi\Phi_s(k)]$. Expanding this at $k \to 0$, one finds

$$f_s(k) = -\tilde C_1 + \frac{|k|}{\gamma} - 0.2393\frac{k^2}{\gamma^2} + O(k^3) \ . \tag{B5}$$

Note that the coefficient in the second term, $|k|/\gamma$, is the same as in Eq.(8.8), which indicates independence of the viscous flow at large scales from directivity of the current injector. However, the limiting value $f_s(k=0)$ is different, 1.505 instead of 1.192, which results in a different value of Sharvin's contact resistance. The $1/x^3$ correction to the edge potential defined by the quadratic term is also non-universal.

Appendix C: Integral representations of the Wiener-Hopf kernels

The Wiener-Hopf analysis given in this text often involve the values of the kernels $K^+_\rho(k,q)$ and $K^+_\Omega(k,q)$ near their poles. In this section, we derive the relevant expression and discuss their long-distance and short-distance behavior. To this end, we first consider a more general kernel:

$$\mathcal{K}_\alpha(q) = 1 - \frac{\alpha}{\sqrt{q^2+\kappa^2}} \ . \tag{C1}$$

The kernel $K_\rho(q)$ is obtained if one takes $\kappa^2 = k^2+\gamma^2$ and $\alpha=\gamma$, while the kernel K_Ω is given by the product of two instances of $\mathcal{K}_\alpha(q)$:

$$K_\rho(k,q) = \mathcal{K}_\gamma(q) \ , \qquad K_\Omega(k,q) = \frac{q^2+\kappa^2}{q^2+k^2}\,\mathcal{K}_\gamma(q)\mathcal{K}_{\gamma'-\gamma''}(q) \ , \tag{C2}$$

so that

$$K^+_\Omega(k,q) = \frac{q+i|k|}{q+i\kappa}\,\mathcal{K}^+_\gamma(q)\,\mathcal{K}^+_{\gamma'-\gamma''}(q) \ . \tag{C3}$$

The kernel $\mathcal{K}_\alpha(q)$ has a zero at $q=i\tilde\kappa$, with $\tilde\kappa=\sqrt{\kappa^2-\alpha^2}$. Let us consider its factor $\mathcal{K}^+_\alpha(is)$ at the imaginary axis. The respective Cauchy integral can be transformed as

$$\log\mathcal{K}^+_\alpha(is) = -\frac{1}{2\pi}\int\limits_{-\infty}^{\infty}\frac{sdq}{s^2+q^2}\,\log\mathcal{K}_\alpha(q) \ . \tag{C4}$$

Since the integral is hard to evaluate, we consider its derivatives with respect to s and α. The Cauchy integral for the log derivative takes the form

$$\frac{d}{ds}\log\mathcal{K}^+_\alpha(is) = -\int\limits_{-\infty}^{\infty}\frac{qdq}{2\pi(q^2+s^2)}\frac{d}{dq}\log\mathcal{K}_\alpha(q) \ , \tag{C5}$$

which can be expanded as

$$\frac{d}{ds}\log\mathcal{K}^+_\alpha(is) = -\frac{\alpha}{2\pi}\int\limits_{-\infty}^{\infty}\frac{q^2dq\left[\alpha+\sqrt{q^2+\kappa^2}\right]}{(q^2+\tilde\kappa^2)(q^2+\kappa^2)(q^2+s^2)} \ . \tag{C6}$$

The first term can be found e.g. by decomposing it into primitive fractions:

$$-\frac{\alpha^2}{2\pi}\int\limits_{-\infty}^{\infty}\frac{q^2dq}{(q^2+s^2)(q^2+\kappa^2)(q^2+\tilde{\kappa}^2)}=-\frac{\alpha^2}{2(\kappa+s)(\tilde{\kappa}+s)(\kappa+\tilde{\kappa})}\ . \tag{C7}$$

The second term can be recast as a difference between two integrals of a similar structure:

$$-\frac{\alpha}{2\pi(s^2-\tilde{\kappa}^2)}\int\limits_{-\infty}^{\infty}\frac{dq}{\sqrt{q^2+\kappa^2}}\left[\frac{s^2}{q^2+s^2}-\frac{\tilde{\kappa}^2}{q^2+\tilde{\kappa}^2}\right]\ . \tag{C8}$$

The integration is facilitated by changing the variable via $q=\kappa\sinh t$ and then $v=\tanh t$, which yields

$$\frac{d}{ds}\log\mathcal{K}_\alpha^+(is)=\frac{1}{2}\frac{d}{ds}\log\frac{s+\kappa}{s+\tilde{\kappa}}-\frac{\alpha}{\pi(s^2-\tilde{\kappa}^2)}\left[\frac{s}{\sqrt{\kappa^2-s^2}}\cos^{-1}\frac{s}{\kappa}-\frac{\tilde{\kappa}}{\alpha}\sin^{-1}\frac{\alpha}{\kappa}\right]\ . \tag{C9}$$

One can, in principle, integrate Eq.(C9) over s to infinity to obtain $\log\mathcal{K}_\alpha(s)$, as $\log\mathcal{K}_\alpha^+(i\infty)=0$.

Another representation of the factorized kernel is obtained if one differentiates it with respect to α:

$$\frac{d}{d\alpha}\log\mathcal{K}_\alpha^+(s)=\int\limits_{-\infty}^{\infty}\frac{s(\alpha+\sqrt{q^2+\kappa^2})}{(q^2+\tilde{\kappa})\,(q^2+s^2)}\frac{dq}{2\pi}\ . \tag{C10}$$

The integrals can be computed as before, and one finds

$$\frac{d}{d\alpha}\log\mathcal{K}_\alpha^+(s)=\frac{\alpha}{2\tilde{\kappa}(s+\tilde{\kappa})}-\frac{1}{\pi}\frac{s}{s^2-\tilde{\kappa}^2}\left[\frac{\sqrt{\kappa^2-s^2}}{s}\cos^{-1}\frac{s}{\kappa}-\frac{\alpha}{\tilde{\kappa}}\sin^{-1}\frac{\alpha}{\kappa}\right]\ . \tag{C11}$$

At $\alpha=0$, $\mathcal{K}_\alpha^+(is)=0$, and one can obtain the kernel by integrating Eq.(C11) over α starting from $\alpha=0$. Employing the relation $\tilde{\kappa}d\tilde{\kappa}=-\alpha d\alpha$, one obtains a representation of the kernel

$$\begin{aligned}\log K_\alpha^+(is)=&\frac{1}{2}\log\frac{s+\kappa}{s+\tilde{\kappa}}+\frac{1}{\pi}\cos^{-1}\frac{s}{\kappa}\tanh^{-1}\frac{\alpha}{\sqrt{\kappa^2-s^2}}-\frac{1}{\pi}\sin^{-1}\frac{\alpha}{\tilde{\kappa}}\tanh^{-1}\frac{s}{\tilde{\kappa}}\\&+\frac{1}{\pi}\int\limits_0^{\alpha}\tanh^{-1}\frac{s}{\sqrt{\kappa^2-\beta^2}}\frac{d\beta}{\sqrt{\kappa^2-\beta^2}}\ .\end{aligned} \tag{C12}$$

These representations can be employed to find the value $\mathcal{K}_\alpha^*$ of $\mathcal{K}_\alpha^*(q)$ at $s=i\tilde{\kappa}$. Instead of applying the general relations, it is more convenient to consider the change of this quantity under a change in α. Since the position of the singularity moves when α is varied, the

derivative of $\log K_\alpha^+(i\tilde\kappa)$ can be found by first differentiating the expression over α at fixed position, and then over s to accomodate for the change in position:

$$\frac{d}{d\alpha}[\log \mathcal{K}_\alpha^+(i\tilde\kappa)] = \frac{d}{d\alpha}\log \mathcal{K}_\alpha^+(is)\bigg|_{s=\tilde\kappa} + \frac{d\tilde\kappa}{d\alpha}\frac{d}{ds}\log \mathcal{K}_\alpha^+(i\tilde\kappa)\ . \tag{C13}$$

Evaluating Eqs.(C11) and (C9), one finds

$$\frac{d}{d\alpha}\log \mathcal{K}_\alpha^+(s)\bigg|_{s=\tilde\kappa} = \frac{\alpha}{4\tilde\kappa^2} + \frac{\kappa^2}{2\pi\alpha\tilde\kappa^2}\sin^{-1}\frac{\alpha}{\kappa} + \frac{1}{2\pi\tilde\kappa}\ , \tag{C14}$$

$$\frac{d}{ds}\log \mathcal{K}_\alpha^+(i\tilde\kappa) = -\frac{\kappa-\tilde\kappa}{4\tilde\kappa(\kappa+\tilde\kappa)} - \frac{\kappa^2}{2\pi\tilde\kappa\alpha^2}\sin^{-1}\frac{\alpha}{\kappa} + \frac{1}{2\pi\alpha}\ . \tag{C15}$$

Using Eqs.(C14) and (C15) and taking into account that $d\tilde\kappa/d\alpha = -\alpha/\tilde\kappa$, one may reduce Eq. (C13) to the form

$$\frac{d}{d\alpha}[\log \mathcal{K}_\alpha^*] = \frac{\alpha}{2\tilde\kappa^2}\frac{\kappa}{(\kappa+\tilde\kappa)} + \frac{\kappa^2}{\pi\alpha\tilde\kappa^2}\sin^{-1}\frac{\alpha}{\kappa}\ , \tag{C16}$$

which can be integrate over α. The first term is evaluated via elementary methods:

$$\frac{\kappa}{2}\int_0^\alpha \frac{\alpha d\alpha}{(\kappa^2-\alpha^2)(\kappa+\sqrt{\kappa^2-\alpha^2})} = \frac{1}{2}\log\frac{\kappa+\sqrt{\kappa^2-\alpha^2}}{2\sqrt{\kappa^2-\alpha^2}}\ . \tag{C17}$$

In the second term, we change the integration variable via $\alpha = \kappa x/\sqrt{1+x^2}$, so that $\sin^{-1}\alpha/\kappa = \tan^{-1}x$. This yields

$$\frac{\kappa^2}{\pi}\int_0^\alpha \frac{d\alpha}{\alpha\tilde\kappa^2}\sin^{-1}\frac{\alpha}{\kappa} = \frac{1}{\pi}\int_0^{x_\alpha}\frac{dx}{x}\tan^{-1}x\ , \tag{C18}$$

where $x_\alpha = \alpha/\sqrt{\kappa^2-\alpha^2}$. Thus, we finally obtain the desired expression:

$$\log \mathcal{K}_\alpha^+(i\tilde\kappa) = \frac{1}{2}\log\frac{\kappa+\sqrt{\kappa^2-\alpha^2}}{2\sqrt{\kappa^2-\alpha^2}} + I(x_\alpha)\ , \qquad I(x_\alpha) \equiv \int_0^{x_\alpha}\frac{dx}{\pi x}\tan^{-1}x\ . \tag{C19}$$

The remaining integral $I(x_\alpha)$ can be expressed in terms of the dilogarithm $\mathrm{Li}_2(x)$. It has an interesting property

$$I(x_\alpha) = I(x_\alpha^{-1}) + \frac{1}{2}\log x_\alpha\ , \tag{C20}$$

which can be verified by splitting the integration domain into two subintervals, $[0,1]$ and $[1,x_\alpha]$ and then changing the integration variable as $y = 1/x$ in the second contribution. This way, one may rewrite Eq.(C19) in an alternative form:

$$\log \mathcal{K}_\alpha^+(i\tilde\kappa) = \frac{1}{2}\log\frac{\alpha(\kappa+\sqrt{\kappa^2-\alpha^2})}{2(\kappa^2-\alpha^2)} + \int_0^{1/x_\alpha}\frac{dx}{\pi x}\tan^{-1}x\ , \tag{C21}$$

which is more suitable if $x_\alpha \gg 1$.

Appendix D: Asymptotic behaviour of the kernels at the pole $q = i|k|$.

Let us now apply the results of the previous section to kernels $K_\rho(k,q)$ and $K_\omega(k,q)$. We begin by considering the long-wavelength limit, $|k| \ll \gamma$, which corresponds to hydrodynamical behaviour. Applying Eq.(C21) to the representation (C2) one finds for the density kernel

$$\log K^*_\rho(k) = \frac{1}{2}\log\frac{\gamma(k+\sqrt{k^2+\gamma^2})}{2k^2} + \frac{1}{\pi}\int\limits_0^{|k|/\gamma}\frac{dx}{x}\tan^{-1}x\ . \tag{D1}$$

In the purely viscous limit, $\gamma'' = 0$, one may also obtain the vorticity kernel in the form

$$\log K^*_\Omega(k,\gamma''=0) = \log\frac{\gamma}{|k|} + \frac{2}{\pi}\int\limits_0^{|k|/\gamma}\frac{dx}{x}\tan^{-1}x\ . \tag{D2}$$

This way, $K^*_{\rho,\Omega}(k)$ can be expanded into Taylor's series in $|k|$, by writing

$$\int\limits_0^{x\ll 1}\frac{dx'}{x'}\ \tan^{-1}x' = x - \frac{x^3}{9} + \frac{x^5}{25} + \dots \tag{D3}$$

Hence one finds

$$\log K^*_\rho(k\to 0) = \log\frac{\gamma}{|k|\sqrt{2}} + \frac{|k|}{\gamma}\left(\frac{1}{\pi}+\frac{1}{2}\right) - \frac{|k|^3}{9\gamma^3}\left(\frac{1}{\pi}+\frac{3}{4}\right) + O(|k|^5)\ , \tag{D4}$$

$$\log K^*_\Omega(k\to 0,\gamma''=0) = \log\frac{\gamma}{|k|} + \frac{2|k|}{\pi\gamma} - \frac{2|k|^3}{9\pi\gamma^3} + O(|k|^5)\ . \tag{D5}$$

For weak ohmic relaxation, $\gamma'' \ll \gamma$, one may approximate $\log K^*_\Omega(k)$ as follows. The factor $\mathcal{K}_{\gamma'-\gamma''}(is)$ in Eq.(C2) is to be evaluated at $s = |k|$ instead of the pole at $\tilde\kappa = \sqrt{k^2+4\gamma'\gamma''}$. For small γ'', the change in $\log\mathcal{K}_{\gamma'-\gamma''}(is)$ can be written in terms of the logarithmic derivative given by Eq.(C15). The respective correction is of the order of $(k-\tilde\kappa)/\gamma$, which can be often neglected. Ignoring this, one can retain γ'' only in the leading logarithmic term:

$$\log K^*_\Omega(k\to 0,\gamma'') \approx \frac{1}{2}\log\frac{\gamma(\gamma'-\gamma'')}{k^2+4\gamma'\gamma''} + \frac{2|k|}{\pi\gamma} + \dots \tag{D6}$$

To obtain the expressions for $K^*_{\rho,\Omega}(k)$ at short distances, $|k| \gg \gamma$, one can employ Eq.(C19). The logarithm yields a quadratic in γ/k, while the integral term yields a first-order term:

$$\log K^*_\rho(k\to\infty) \approx \frac{\gamma}{|k|} + \frac{\gamma^2}{8k^2} + O(|k|^{-3})\ , \tag{D7}$$

$$\log K^*_\Omega(k\to\infty) \approx \frac{2\gamma'}{|k|} + O(k^{-2})\ .$$

Appendix E: The uniform-flow limit.

Uniform flows, such as Poiseuille flow, are described by the limit $k = 0$. Let us find $K^+_\Omega(k, is)$ at small but finite $s \to 0$, i.e., $|k| \ll s \ll \gamma$. Using the representation (C12) and the factorisation (C2) and setting $\kappa = \alpha = \gamma$, $\tilde{\kappa} = k = 0$, we write

$$\log K^+_\Omega(0,s) = \frac{1}{\pi}\cos^{-1}\frac{s}{\gamma}\log\frac{\gamma+\sqrt{\gamma^2-s^2}}{\gamma-\sqrt{\gamma^2-s^2}} + \frac{1}{\pi}\int\limits_0^\gamma \frac{d\alpha}{\sqrt{\gamma^2-\alpha^2}}\log\frac{\sqrt{\gamma^2-\alpha^2}+s}{\sqrt{\gamma^2-\alpha^2}-s}\ . \qquad \text{(E1)}$$

In the first two terms one can make Taylor expansion in s/γ. As to the remaining integral, s can be treated as a small parameter almost everywhere in the integration domain except for small region $\gamma \approx \alpha$. Hence we split the integration variable $x = \sqrt{\gamma^2-\alpha^2}$:

$$\log K^+_\Omega(0,s) = \frac{1}{\pi}\left(\frac{\pi}{2}-\frac{s}{\gamma}\right)\log\frac{4\gamma^2}{s^2} + \frac{1}{\pi}\int\limits_0^\gamma \frac{dx}{\sqrt{\gamma^2-x^2}}\log\frac{x+s}{x-s}\ , \qquad \text{(E2)}$$

and split the integration range $(0,\gamma)$ into two segments: $(0,x_0)$ and (x_0,γ), choosing the split point x_0 such that $s \ll x_0 \ll \gamma$. In the integral over $(0,x_0)$ one may neglect the square root, while in the integral over (x_0,γ) one may make an expansion in s/γ:

$$log K^+_\Omega(0,s) = \left(1-\frac{2s}{\pi\gamma}\right)\log\frac{2\gamma}{s} + \frac{1}{\pi}\int\limits_0^{x_0} dx\ \log\frac{x+s}{x-s} + \frac{2s}{\pi}\int\limits_{x_0}^{\gamma}\frac{dx}{x\sqrt{\gamma^2-x^2}}\ . \qquad \text{(E3)}$$

Computing the integrals and making the approximations $s \gg x_0$ and $x_0 \ll \gamma$, one finds

$$\log K^+_\Omega(0,s) = \left(1-\frac{2s}{\pi\gamma}\right)\log\frac{2\gamma}{s} + \frac{2s}{\pi\gamma}\log\frac{x_0}{s} + \frac{2s}{\pi\gamma} + \frac{2s}{\pi\gamma}\log\frac{2\gamma}{x_0}\ . \qquad \text{(E4)}$$

We now see that the split point x_0 drops out, and one obtains

$$\log K^+_\Omega(0,s) = \log\frac{2\gamma}{s} + \frac{2s}{\pi\gamma} + O(s^2)\ . \qquad \text{(E5)}$$

Exponentiating this expression, we finally write

$$\log K^+_\Omega(0,s) = \frac{2\gamma}{s} + \frac{4}{\pi\gamma}\ . \qquad \text{(E6)}$$

Check factors of two!

The Cauchy integral takes the form

$$\log K^+_\Omega(is) = -\frac{2}{\pi}\int\limits_0^\infty \frac{sdq}{s^2+q^2}\log\frac{\sqrt{q^2+\gamma^2}-\gamma}{q}\ . \qquad \text{(E7)}$$

To calculate the integral retaining the regular part of $K_\Omega(0,q)$, we split the integration range into two: $[0,q_0]$ and $[q_0,\infty]$, where $s \ll q_0 \ll \gamma$. For $q < q_0$, we can rewrite the argument of the logarithm as $|q|/(2\gamma)$. For $q > q_0$, s^2 in the denominator can be neglected:

$$\log K^+_\Omega(is) = -\frac{2}{\pi}\int\limits_0^{q_0} \frac{sdq}{q^2+s^2}\log\frac{q}{2\gamma} - \frac{2}{\pi}\int\limits_{q_0}^{\infty}\frac{sdq}{q^2}\log\frac{\sqrt{q^2+\gamma^2}-\gamma}{q} \ . \tag{E8}$$

Using the well-known relation[10]

$$\int\limits_0^{\infty}\frac{dq}{q^2+a^2}\log\frac{q}{b} = \frac{\pi}{2|a|}\log\frac{|a|}{b} \ , \tag{E9}$$

we find

$$\log K^+_\Omega(is) = \log\frac{2\gamma}{q} - \frac{2s}{\pi}\int\limits_{q_0}^{\infty}\frac{dq}{q^2}\log\frac{2\gamma\left(\sqrt{\gamma^2+q^2}-\gamma\right)}{q^2} \ . \tag{E10}$$

The remaining integral can be found via integration by parts, which gives

$$\int\limits_{q_0}^{\infty}\frac{dq}{q^2}\log\frac{\sqrt{\gamma^2+q^2}-\gamma}{2\gamma} = \left[-\frac{1}{q}\log\frac{2\gamma\left(\sqrt{q^2+\gamma^2}-\gamma\right)}{q^2} + \frac{1}{q} - \sqrt{\frac{1}{\gamma^2}+\frac{1}{q^2}}\right]_{q_0}^{\infty} \approx -\frac{1}{\gamma} \ . \tag{E11}$$

Hence

$$K^+_\Omega(0,is) \approx \frac{2\gamma}{s}\exp\left(\frac{2s}{\pi\gamma}\right) \approx \frac{2\gamma}{s} + \frac{4}{\pi} \ . \tag{E12}$$

Appendix F: Expressions for potential and stream function

Expressions (8.4) and (8.6) can be rewritten by explicitly separating the contribution of long-lived hydrodynamical modes and short-lived higher-order harmonics. This is achieved by deforming the contour C_+ shown in Fig. 2 into two contours enclosing the pole and the cut. Evaluating the integrand, one can make use of the following facts. Firstly, it is possible to express all quantities in terms of a single function, since $K^-_\rho(k,-is) = 1/K^+_\rho(k,is)$. Secondly, the behaviour near the poles can be extracted from Eq. (4.1):

$$K^+_\rho(k,-is) = \frac{1}{K_\rho(k,-is)K^-(k,-is)} = \frac{1}{K_\rho(k,-is)K^+_\rho(k,is)} \ . \tag{F1}$$

Near the pole $q = -i|k|$, one finds This yields e.g.

$$K^+_\rho(q \approx -i|k|) = -\frac{\gamma^2}{|k|(|k|-iq)K^*_\rho(k)} \ , \tag{F2}$$

where $K^*_\rho(k) \equiv K^+_\rho(k, i|k|)$ as usual. With this in mind, one can write the pole contribution to the potential by employing Eqs.(6.7) and (7.4):

$$\delta\phi_{\rm pole}(x,y) = \int\limits_{-\infty}^{\infty} \frac{dk}{2\pi} e^{-ikx-|k|y} \left\{ I_0 \left[\frac{\gamma'\gamma^2}{2k^3\left[K^*_\rho(k)\right]^2} - \frac{\gamma'}{|k|} + \frac{2\gamma}{|k|K^*_\rho(k)} \right] \right. \\ \left. + \frac{f_s(k)}{2}\left[1 + \frac{\gamma^2}{2k^2\left[K^*_\rho(k)\right]^2}\right]\right\} . \tag{F3}$$

To compute the branch cut contribution, we note that the integrals over the branch cut are only sensitive to the square root singularity, as the contributions continuous across the cut cancel. Hence, at the branch cut one can retain only singular contributions to the kernels, replacing $K^+_\rho(k,-is)$ by its discontinuity across the cut

$$\Delta \frac{1}{K^+_\rho(-is)} = \frac{2\gamma\sqrt{s^2-\kappa^2}}{(s^2-k^2)K^+_\rho(is)} . \tag{F4}$$

This transforms the respective terms in the potential to the form

$$\delta\phi_{\rm cut}(x,y) = \int\limits_{-\infty}^{\infty} \frac{dk}{2\pi}\, e^{-ikx} \int\limits_{\sqrt{k^2+\gamma^2}}^{\infty} e^{-sy}\frac{ds}{\pi} \frac{\sqrt{s^2-k^2-\gamma^2}}{(s^2-k^2)K^+_\rho(k,is)} \left\{ \frac{\gamma f_s(k)}{2(|k|+s)K^*_\rho(k)} \right. \\ \left. + I_0\left[\frac{\gamma\gamma'}{|k|(|k|+s)K^*_\rho(k)} + 2 - \frac{2(s^2-k^2)K^+_\rho(k,is)}{s^2-\gamma^2-k^2}\right]\right\} . \tag{F5}$$

The resulting potential can be now written in the form

$$\phi(\boldsymbol{r}) = \frac{I_0}{\pi|\boldsymbol{r}|} e^{-\gamma|\boldsymbol{r}|} + \delta\phi_{\rm pole}(\boldsymbol{r}) + \delta\phi_{\rm cut}(\boldsymbol{r}) . \tag{F6}$$

The pole contribution depends upon distance via the factor $\exp(-ikx-|k|y)$ and hence obeys Laplace's equation: $\nabla^2\phi_{\rm pole}(\boldsymbol{r}) = 0$. At large scale, it produces a slow-decaying contribution $\propto |\boldsymbol{r}|^{-2}$ which represents hydrodynamical pressure. The cut contribution $\delta\phi_{\rm cut}(\boldsymbol{r})$ decays as $\exp(-\gamma y)$ or faster, and hence represent short-lived ballistic modes.

To recast the stream function (8.6) into a similar form, one can rewrite $K^+_\Omega(k,-is)$ in a similar form:

$$K^+_\Omega(k,-is) = \frac{k^2-s^2+2i\gamma'\sqrt{s^2-\gamma^2-k^2}+2\gamma\gamma'}{(k^2+4\gamma'\gamma''-s^2)K^+_\Omega(k,is)} . \tag{F7}$$

The integrand in Eq. (8.6) therefore has two poles: at $q = -i|k|$ and at $q = -i\tilde\kappa = -i\sqrt{k^2+4\gamma'\gamma''}$. Near the poles, one finds

$$K^+_\Omega(k,i|k|) = \frac{\gamma}{\gamma'' K^*_\Omega(k)} , \qquad K^+_\Omega(k, q\approx -i\tilde\kappa) = \frac{1}{q+i\tilde\kappa}\frac{2i\gamma'(\gamma'-\gamma'')}{\tilde\kappa K^+_\Omega(k,i\tilde\kappa)} . \tag{F8}$$

Therefore, the pole contribution takes the form

$$\Psi_{\rm pole}(x,y) = \int\limits_{-\infty}^{\infty} \frac{dk}{2\pi}\, e^{-ikx} \left\{ \frac{i\,\mathrm{sgn}\,k}{4\gamma''\gamma'} \left[f_s(k) + \frac{2\gamma'}{|k|} I_0 \right] e^{-|k|y} \right. \tag{F9}$$
$$\left. \times \left[\frac{\gamma}{[K^*_\Omega(k)]^2} - \gamma'' - \frac{(\gamma'-\gamma'')|k|}{\sqrt{k^2+4\gamma'\gamma''}} \frac{1}{K^*_\Omega(k) K_\Omega(k, i\tilde{\kappa})} e^{-(\tilde{\kappa}-|k|)y} \right] \right\} .$$

Using the discontinuity of $K^+_\Omega(k,-is)$,

$$\Delta K^+_\Omega(k,-is) = -\frac{4i\gamma'\sqrt{s^2-k^2-\gamma^2}}{(s^2-k^2-4\gamma'\gamma'')K^+_\Omega(k,is)} , \tag{F10}$$

one finds the cut contribution:

$$\Psi_{\rm cut}(x,y) = i\gamma' \int\limits_{-\infty}^{\infty} \frac{dk}{2\pi}\, e^{-ikx} \int\limits_{\sqrt{k^2+\gamma^2}}^{\infty} \frac{ds}{\pi} \left[\frac{k f_s}{\gamma'} + 2I_0 \right] \frac{\sqrt{s^2-k^2-\gamma^2}}{(s^2-k^2-4\gamma'\gamma'')} \frac{e^{-sy}}{s^2-k^2} . \tag{F11}$$

The full stream function is given by

$$\Psi(\boldsymbol{r}) = \frac{I_0}{\pi} \tan^{-1}\frac{y}{x} + \Psi_{\rm pole}(\boldsymbol{r}) + \Psi_{\rm cut}(\boldsymbol{r}) . \tag{F12}$$

The pole contribution obeys the generalised Ohm-Stokes law, $[\nabla^4 - 4\gamma'\gamma''\nabla^2]\,\Psi_{\rm pole}(x,y) = 0$. In the purely viscous case ($\gamma'' = 0$) this equation is reduced to a biharmonic equation, and the two poles in $\Psi_{\rm pole}(x,y)$ merge together. In this limit, one may expand $\Psi_{\rm pole}(x,y)$ to the lowest order in γ'', which yields

$$\Psi_{\rm pole}(x,y) = \int\limits_{-\infty}^{\infty} \frac{dk}{2\pi}\, e^{-ikx} \left\{ \frac{i\,\mathrm{sgn}\,k}{2\,[K^*_\Omega(k)]^2} \left[f_s(k) + \frac{2\gamma'}{|k|} I_0 \right] e^{-|k|y} \right. \tag{F13}$$
$$\left. \times \left[-\frac{1}{2}\,[K^*_\Omega(k)]^2 + 1 + \frac{\gamma^2}{k^2} + \frac{\gamma^2 y}{|k|} + \frac{\gamma^2}{|k|} K'_\Omega(k) \right] \right\} ,$$

where $K'_\Omega(k)$ is the logarithmic derivative of $K_\Omega(k,q)$ at $q = i|k|$, which can be found from (C15):

$$K'_\Omega(k) = \frac{1}{\pi\gamma} - \frac{k^2+\gamma^2}{\pi k\gamma^2} \tan^{-1}\frac{\gamma}{|k|} \tag{F14}$$

A similar expression for K^+_Ω is often needed to the next order, due to the double poles in the expression for the current components $j_{x,y}$:

$$K^+_\Omega(q \approx -i\tilde{\kappa}) = -\frac{2\gamma'(\gamma'-\gamma'')}{\tilde{\kappa}\tilde{K}^*_\Omega} \frac{1}{\tilde{\kappa} - iq} , \tag{F15}$$

with $\tilde{K}^*_\Omega \equiv K^+_\Omega(k, i\tilde{\kappa})$. In the viscous limit, the next leading term in the expansion is also to be retained:

$$K^+_\Omega(q \approx -i|k|) = -\frac{2\gamma^2}{|k|K^*_\Omega}\left[\frac{1}{|k|-iq} + \frac{1}{2|k|} + \frac{|k|}{\gamma^2} - K'_\Omega\right] , \tag{F16}$$

where K'_Ω is the log-derivative, $K'_\Omega \equiv \frac{d}{ds}\log K^+_\Omega(is)$ at $s = |k|$, and $K^*_\Omega \equiv K^+_\Omega(k, i|k|)$. The quantities $K^*_{\rho,\Omega}(k)$ and $K'_\Omega(k)$ are discussed in Appendix D.

Finally, integrals over the branch cut are only sensitive to the square root singularity, as the contributions continuous across the cut cancel. Hence, at the branch cut one can retain only singular contributions to the kernels, making the replacement

$$\frac{1}{K^+_\rho(-is)} \to \frac{\gamma\sqrt{s^2-\kappa^2}}{(s^2-k^2)K^+_\rho(is)} , \qquad \frac{1}{K^+_\Omega(-is)} \to \frac{2\gamma'\sqrt{s^2-\kappa^2}}{(s^2-\tilde{\kappa}^2)K^+_\Omega(is)} . \tag{F17}$$

---

[1] Ref to collision integral

[2] Wiener-Hopf (Noble?)

[3] Reuter-Sondheimer

[4] Shytov et al

[5] Levitov-Falkovich

[6] Scanning gate measurements: Ilani?

[7] Vicinity resistance measurements.

[8] Ensslin, scanning gate measurements

[9] Measuring psi: Levitov-Falkovich theorem, Ilani's measurements

[10] Gradstein and Ryzhik, the integral $log(x)/(x^2+a^2)$